Multifunctional thiosemicarbazones targeting sigma receptors: in vitro and in vivo antitumor activities in pancreatic cancer models

Multifunctional thiosemicarbazones targeting sigma receptors: *in vitro* and *in vivo* antitumor activity in adenocarcinoma pancreatic models

Mauro Niso[a#], Joanna Kopecka[b#], Francesca Serena Abatematteo[a], , Francesco Berardi[a], Chiara Riganti[b*], Carmen Abate[a*]

[a]Università degli Studi di Bari ALDO MORO, Dipartimento di Farmacia-Scienze del Farmaco, Via Orabona 4, 70125 Bari.

[b]Department of Oncology, University of Turin, via Santena 5/bis, 10126, Torino, Italy

[#]Equally Contributing Authors

[*]Corresponding Authors

Chiara Riganti, via Santena 5/bis, 10126, Torino, Italy, +390116705857, chiara.riganti@unito.it

Carmen Abate, via Orabona 4, 70125, Bari, Italy, +390805442231, carmen.abate@uniba.it

Abstract

Purpose: The association of the metal chelating portion of thiosemicarbazone with the cytotoxic activity of sigma-2 receptors appears as a promising strategy in pancreatic tumors. Therefore, we developed a novel sigma-2 receptor targeting thiosemicarbazone (**FA4**) that incorporates a moiety associated with lysosome destabilization and ROS increase in order to develop more efficient antitumor agents.

Methods: The density of sigma receptors was evaluated in pancreatic cells by flow cytometry analyses. In these cells, cytotoxicity (MTT assay) and the activation of the ER and mitochondria -dependent (mRNA expression of GRP78, ATF6, IRE1, PERK; ROS levels by MitoSOX and DCFDA-AM; JC-1 staining) cell death pathways induced by thiosemicarbazones **FA4**, **MLP44**, **PS3** and **ACthio-1**, were evaluated. Autophagic proteins (ATG5, ATG7, ATG12, beclin, p62 and LC3-I) were also studied. *In vivo* effect of **FA4** in xenografts was investigated and challenged with gemcitabine.

Results: FA4 exerted more potent cytotoxicity than the previously studied thiosemicarbazones (**MLP44**, **PS3** and **ACthio-1**) which displayed variable effects on the ER or mitochondria -dependent pro-apoptotic axis. By contrast, **FA4** always activated pro-apoptotic pathways and decreased autophagy, except for MiaPaCa2 cells, where autophagy proteins were less expressed and unmodified by **FA4**. Treatment of PANC-1 mice models, poorly responsive to conventional chemotherapy, with **FA4** significantly reduced tumor volume and increased intratumor apoptosis compared to gemcitabine, with no signs of toxicity.

Conclusion: Altogether, **FA4** that shows encouraging activity in cells unresponsive to gemcitabine, deserves further investigation in patient-derived pancreatic adenocarcinomas, while the results obtained held promises for the development of therapies that can more efficiently target the peculiar characteristics of each tumor type.

Keywords: Thiosemicarbazone, adenocarcinoma pancreatic tumor, sigma receptors, caspase 3/7/9, autophagy, PANC-1 xenograft.

Introduction

Pancreatic tumor is one of the most aggressive cancers characterized by a very poor prognosis and a five-years survival rate around 8%. While the overall cancer death rate has constantly declined over the past two decades for the four major cancers (lung, breast, prostate, and colorectum), death rates increased for pancreatic cancers. [1] Surgery represents the first option when the disease is early diagnosed, with gemcitabine as the chemotherapeutic agent towards which cancer cells ultimately develop resistance. Therefore, there is an urgent need for alternative therapeutic strategies to face such harmful disease. With this aim, we previously produced a series of thiosemicarbazones that chelate metals and display activity towards the sigma-2 receptors and the drug efflux pump P-glycoprotein (P-gp). [2] The strategy to simultaneously hit these targets against pancreatic cancer was based on diverse pieces of evidence: 1) some sigma-2 receptor ligands are effective against pancreatic tumors [3–7]; 2) cancer cells are sensitive to changes in energy levels because of their increased energy need to support rapid cell proliferation. [8] Interaction with the subtype 2 of sigma receptors, that are overexpressed in several tumors, activates apoptotic pathways that depend on the cell type and on the molecule type. [9] Upon metal (iron and copper) chelation, thiosemicarbazones are able to alter the cell energy equilibrium. In the attempt to link these two activities, potent cytotoxic thiosemicarbazones that bind sigma-2 receptor were obtained and the impact to the synergistic action of the biological targets hit by these molecules (i.e sigma-2 receptors, efflux pumps like P-gp and metal chelation) was studied through a deconstruction approach (Figure 1). We evaluated the activity of these molecules in an *in vivo* preclinical model of pancreatic cancer. [4] We showed that while the multitarget strategy is not needed for the antitumor activity (the sole *N*,*N*-dimethylthiosemicarbazone chelating moiety is sufficient to confer cytotoxic action, as in compound **ACthio-1**, (*Z*)-*N*,*N*-dimethyl-2-(2-oxoindolin-3-ylidene)hydrazinecarbothioamide, Figure 1), the presence of the sigma-

2 targeting portion (as in compounds **MLP44**, (*Z*)-2-(1-(4-(6,7-dimethoxy-3,4-dihydroisoquinolin-2(1*H*)-yl)butyl)-2-oxoindolin-3-ylidene)-*N*,*N*-dimethylhydrazinecarbothioamide and **PS3**, (*Z*)-2-[1-[4-(4-cyclohexylpiperazin-1-yl)butyl]-2-oxoindolin-3-ylidene]-*N*,*N*-dimethylhydrazinecarbothioamide, Figure 1) could result in diverse cell death pathways and in a more specific delivery to tumors, leading to reduced off-targets effects. [4] These promising results prompted us to produce a novel sigma-2 binding thiosemicarbazone, whose sigma-2 binding basic moiety was the 3*H*-spiro[isobenzofuran-1,4'-piperidine]. The overall structure mimicked the sigma-2 reference compound siramesine, which was shown to be cytotoxic in a number of cells via pathways such as lysosomal leakage [10] and mitochondria destabilization [11] that lead to oxidative stress. [10–12] Insertion of such a moiety could result in an increased cytotoxic effect in pancreatic cancer cells, by combining the potent action of the sigma-2 ligand siramesine with the metal chelating moiety proper of the thiosemicarbazone within one scaffold. This novel compound named **FA4**, (*Z*)-2-(1-(4-(3*H*-spiro[isobenzofuran-1,4'-piperidine]-1'-yl)butyl)-2-oxoindolin-3-ylidene)-*N*,*N*-dimethylhydrazinecarbothioamide (Figure 1), was studied in a panel of pancreatic cancer cells and challenged with our most promising thiosemicarbazones, either targeting sigma-2 receptors (**MLP44** and **PS3**) or not (**ACthio-1**). While all the thiosemicarbazones studied are cytotoxic in the diverse pancreatic cancer cells, the type/presence of the basic moiety triggers different pathways in the diverse cells, a result that looks promising in the perspective of a personalized medicine approach. Additionally, the novel compound performed better than the other thiosemicarbazones in all the pancreatic tumor cell lines, with important cytotoxic action in the human aggressive PANC-1 cells, which display a reduced sensitivity to the first-line treatment gemcitabine against which they eventually develop resistance. [13] The in vitro results were also confirmed in PANC-1 xenografts shedding light on the potentials of **FA4** in the treatment of pancreatic tumors.

Results

Chemistry

According to a previously set up procedure, **FA4** was synthesized starting from the alkylation of the 3*H*-spiro[isobenzofuran-1,4'-piperidine] [14] with 1-(4-chlorobutyl)indoline-2,3-dione **1** in the presence of K_2CO_3, [2] providing the amine **2**. This intermediate amine was transformed into its corresponding hydrochloride salt, dissolved in hot EtOH and treated with 4,4-dimethyl-3-thiosemicarbazide to afford final thiosemicarbazone **FA4** as hydrochloride salt (Scheme S1, Supplementary Information). The synthetic experimental procedures are reported in the Supplementary Information.

Affinity of FA4 at the sigma-2 receptors by radioligand binding assay

The binding of **FA4** at sigma-2 receptors measured through by classical radioligand binding assay was notable (K_i = 15.8 nM, Table 1) and in strict agreement with the binding affinity of the siramesine lead compound (K_i = 12.6 nM) [8] showing how the thiosemicarbazone moiety was not detrimental for the sigma-2 receptor binding.

Density of sigma-2 receptors and binding affinity of FA4 in tumor and normal (immortalized) pancreatic cells

The presence of sigma-2 receptors was evaluated in a panel of pancreatic cells. Flow cytometry analyses in the human (MiaPaCa2, PANC-1, AsPC1 and BxPC3) and murine (KP02, PANC02) adenocarcinoma pancreas cells together with HPDE cells were conducted for this aim. The assay was performed by incubating each cell line with increasing concentrations of the selective sigma-2 fluorescent ligand **NO1**. [15,16] Saturation of the sigma-2 receptors in each cell line and definition of the non-specific binding through displacement with DTG led to define the specific binding. Results clearly indicate that sigma-2 receptors are from 1.8- to 3.2-fold more expressed in adenocarcinoma pancreatic cells than in HPDE cells (Figure S1 – A, Supplementary Information). The only exception is the KP02 cell line in which the density of sigma-2 receptors is comparable to the density in HPDE

cells. By means of the flow cytometry, we measured the binding affinity of **FA4** at sigma-2 receptor subtypes in the pancreatic cells according to the previously set up procedures. [15] Binding curves were generated for the thiosemicarbazone, upon dose-dependent displacement of the fluorescent ligand **NO1** [15] with **FA4** leading to IC_{50} values that line up with the results from the radioligand binding assay (IC_{50} values ranging from 9.13 nM to 11.6 nM in MiaPaCa2, PANC-1, Aspc1 and KP02, Table 1), showing an equally high nanomolar affinity in these representative cell lines.

Density of sigma-1 receptors and binding affinity of FA4 in tumor and normal (immortalized) pancreatic cells

Because in our hands siramesine binds equally well the sigma-1 and sigma-2 receptor subtypes, [8] we investigated the presence of sigma-1 receptors together with the binding of **FA4** for this subtype in the clinically relevant pancreatic cancer cells (PANC-1 and MiaPaCa2). The sigma-1 fluorescent ligand **LM1** [17] was used to measure the sigma-1 receptor density in the above cells and HPDE cells upon masking of the sigma-2 subtype with the selective sigma-2 ligand **F390** [18] (Figure S1 – B, Supplementary Information). The presence of the sigma-1 receptor was ascertained, with no difference in the amount between the tumor and immortalized cells, in contrast to the sigma-2 receptor. Additionally, the binding curves generated upon dose-dependent displacement of **LM1** in PANC-1 and Miapaca-2 led to define a moderate affinity of **FA4** for sigma-1 receptors (IC_{50} values = 51.3 and 53.2 nM, respectively, Table 1), suggesting a more pronounced sigma-2 than sigma-1 mediated action of **FA4** in the biological assays.

Cytotoxic activity of FA4 in tumor and normal (immortalized) pancreatic cells

The cytotoxic activity of the novel thiosemicarbazone **FA4** was evaluated in human (MiaPaCa2, and PANC-1, AsPC1 and BxPC3,) and murine (KP02, PANC02) pancreatic adenocarcinoma cells with diverse driver mutations (Table 2). **FA4** demonstrated relevant low micromolar cytotoxic activity in all the cell lines studied (EC_{50} ranging from 0.88 μM to 3.01 μM, Table 2). In particular, in PANC-

1, MiaPaCa2 and KP02 cells, **FA4** activity was from 3- to 8-fold higher compared to the cytotoxicity conferred by the other sigma-2 targeting thiosemicarbazones **MLP44** and **PS3**. Cytotoxicity of all thiosemicarbazones was also measured in HPDE cells where the compounds generally showed a less potent activity than in the adenocarcinoma cells, but again, only **FA4** consistently displayed a 2- to 7- fold lower cytotoxicity (EC_{50} = 6.11, Table 2).

FA4 induces cell apoptosis by eliciting endoplasmic reticulum stress and mitochondrial damage

First, we investigated whether the compounds induced apoptosis, an effect that has been already reported for sigma-2 receptors ligands in cancer cells. [3,19,20] We first measured the activity of caspase 3, i.e. the caspase that irreversibly determines apoptotic death, in human MiaPaCa2, PANC-1, and AspC1 and in murine KP02 and PANC02 cells, treated with sigma-2 targeting thiosemicarbazones **FA4**, **MLP44**, **PS3**, and metal chelator **ACthio-1** (Figure 2), in the same experimental conditions (50 μM for 2 h) in which sigma-2 receptors ligands induced cytotoxic effects against pancreatic cancer cells [3]. **FA4** activated caspase 3 in all the cell lines investigated, while the other compounds activated caspase 3 in a variable and cell-dependent manner. For instance, the other thiosemicarbazones did not activate caspase 3 in MiaPaCa2 and AspC1, but they activated caspase 3 in murine PANC02 and KP02 cells, in partial agreement with previous findings. [4]

Moreover, **FA4** was the most potent inducer of caspase 3 in all cell lines compared to the other compounds (with the only exception of **ACthio-1** having similar activity in KP02).

Notably, **FA4** was a significant inducer of caspases in all the cell lines analyzed, except for MiaPaCa2 cells, also when used at the concentration corresponding to its IC50 in each cell line (Supplementary Figure S2).

To better investigate the biochemical mechanisms of **FA4** and the other compounds in inducing apoptosis, we first focused on the effects exerted on endoplasmic reticulum (ER), an intracellular compartment where sigma-2 receptors have been reported. [21]

Sigma-2 receptors are known inducers of ER stress, a condition that perturbs the correct folding of proteins within the ER and causes the so-called unfolded protein response (UPR). UPR is sensed by the chaperone glucose-regulated protein 78 (GRP78) and by the sensors activating factor 6 (ATF6), inositol-requiring enzyme-1α (IRE-1α) and PKR-like ER kinase (PERK) that activate downstream effectors leading to cell survival if the ER stress is short and reversible, or cell apoptosis by activating the caspase 7/caspase 3 axis if the stress persists. [22] By altering calcium flux, sigma-2 receptors modulators are known to induce ER stress [23] and promote cell death by activating apoptotic and autophagic pathways. [24]

The mRNA expression of ER stress markers such as GRP78, ATF6, IRE1 and PERK were evaluated in all the pancreatic cancer cells studied (Figure 3A). The four ER stress markers increased upon treatment with **FA4** in all the cells except for MiaPaCa2 cells. All the thiosemicarbazones increased the mRNA expression of these markers in PANC-1, whereas none of the markers was increased in the other cells by **MLP44**, **PS3** and **ACthio-1**. The increase of ER stress induced by FA4 was validated by the immunoblotting of GRP78, ATF6, IRE1 and PERK (Figure 3B): the results confirmed that in all cell lines except MiaPaCa2, this thiosemicarbazone was able to increase the expression of ER stress sensors and executers. Notably, **FA4** increased the expression of ER stress markers also when used at its IC50 concentration (Supplementary Figure S3). In agreement with the ER stress markers gene expression modulation, caspase 7, which is activated upon ER stress, was activated by **FA4** in all cell lines except for MiaPaCa2 cells (Figure 2, Supplementary Figure S2). Similarly, all the thiosemicarbazones increased caspase 7 in PANC-1 cells, while the behavior in the other cell lines was highly variable. The activation of caspase 7 may be responsible for the activation of the downstream caspase 3, although the extent of caspase 7 and caspase 3 activation are not always comparable in the same cell lines treated with the same compound. These small discrepancies may be due to different pool of pro-apoptotic and anti-apoptotic factors that each cell line has and may be affected differently by the compounds. Alternatively, other mechanisms converging on the activation of caspase 3 could be hypothesized.

198 The alteration of calcium homeostasis in the so-called Mitochondria-associated ER membranes
199 (MAM) also alters mitochondria metabolic functions, leading to calcium overload, increased
200 production of reactive oxygen species (ROS), mitochondrial depolarization followed by the activation
201 of cell death triggered by caspase 9/caspase 3 axis and autophagy. [25] Importantly, sigma receptors,
202 have been found in the MAM cell compartments, where in particular the sigma-1 subtype regulates
203 Ca^{2+} fluxes between the ER and mitochondria. [26]
204 We thus focused on mitochondria-related events as possible triggers of additional pro-apoptotic
205 mechanisms. Interestingly, **FA4** increased mitochondrial ROS in all the cell lines except for
206 MiaPaCa2, whereas the other thiosemicarbazones increased mitochondrial ROS only in PANC-1 and
207 PANC02 (Figure 4). The levels of ROS in whole cells (Figure 4) reflected the levels of mitochondrial
208 ROS, suggesting that ROS can diffuse from mitochondria to cytosol. Alternatively, we may speculate
209 that thiosemicarbazones are able to increase ROS also in a mitochondria-independent way, e.g. by
210 increasing cytosolic ROS-producing enzymes such as NADPH oxidase or reducing the activity of
211 anti-oxidant enzymes, such as superoxide dismutase 1, catalase, peroxidases, thioredoxins.
212 Preliminary data on the activity of NADPH oxidase, superoxide dismutase 1 and catalase
213 (Supplementary Figure S4), however, seems to exclude this second hypothesis.
214 The increase in mitochondrial ROS was harmful in treated cancer cells. Indeed, the staining with JC1,
215 a dye sensitive to the mitochondrial depolarization, indicated that all **FA4**-treated cells had
216 depolarized (i.e. damaged) mitochondria, except for MiaPaCa2 (Figure 4). The other
217 thiosemicarbazones increased mitochondria depolarization only in PANC-1 and PANC02 cells, not
218 in the other cell lines (Figure 4). This parallelism between mitochondrial ROS and depolarization
219 suggests that the latter event is consequent to the increased mitochondrial ROS. Mitochondria damage
220 triggers the activation of caspase 9, and this event was observed in all the cells where **FA4** increased
221 mitochondrial ROS and depolarization (Figure 2,4). By contrast, the other compounds had a variable
222 activation of the caspase, dependent on the cell line and not strictly correlated with mitochondrial

ROS and depolarization. Again, MiaPaCa2 cells were completely refractory to the activation of caspase 9 (Figure 2).

As proof of concept that mitochondrial ROS triggered the cell death induced by **FA4**, we treated cells with the mitochondrial ROS scavenger mitoquinol (mitoQ), at a concentration that abrogated the increase of mitochondrial ROS elicited by FA4 (**Figure 5A**): in these experimental condition we did not find any activation of caspase 9 and caspase 3 in **FA4**-treated cells (**Figure 5B-C**).

To explain the absence of activation of ER stress- and mitochondrial stress-dependent pro-apoptotic pathways in MiaPaCa2 cells, in contrast with the other cell lines, we investigated whether cells differ for autophagy that contributes to the apoptosis induced by sigma-2 receptors following ER [24] or mitochondrial [25] stress. Interestingly, all PDAC responsive cell lines have higher levels of autophagosome proteins (ATG5, ATG7, ATG12, beclin 1), sequestration markers (p62) and LC3-II/LC3-I ratio than MiaPaCa2 cells. Moreover, **FA4** reduced the levels of all the above-mentioned protein and the LC-I/LC-II conversion in responsive cells but not in MiaPaCa2 cells (Figure 6).

***In vivo* antitumor activity of FA4**

The potent in vitro antitumor activity shown by **FA4** in the aggressive human PANC-1 cells prompted us to investigate whether the anticancer effect is translated in vivo as well. In a first experiment, PANC-1 and MiaPaCa2 xenografts were treated for 15 days with two dosages (^{low} and ^{high}) of **FA4**, following the protocol adopted for other thiosemicarbazones. [4] Gemcitabine was used as comparison, because it is the standard treatment in pancreatic cancers. At the end of the treatments, tumors were significantly smaller for mice treated with FA4 750 ^{low} and FA4 1500 ^{high} compared to vehicle in PANC-1 xenografts. An important reduction in tumor volume for both **FA4** regimens was also recorded in PANC-1 tumors in comparison with mice treated twice weekly by gemcitabine that was ineffective against this tumor cell line (Figure S5A, Supplementary Information). By contrast, MiaPaCa2 tumors were more sensitive to gemcitabine, but- in line with the data observed *in vitro* - **FA4** was ineffective at both dosages (Figure S5B, Supplementary Information).

In a second experimental set, we prolonged the treatment of PANC-1 tumor-bearing animals for 30 days, to evaluate the effects in terms of tumor growth rate and systemic toxicity. In these conditions, while gemcitabine was not able to reduce significantly tumor growth, **FA4** at the low dosage showed a cytostatic effect and **FA4** at higher dosages a regression of tumor growth (Figure 7A-B). Moreover, in line with the apoptosis and the increased ROS observed in PANC-1 cells, the intratumor apoptosis, measured as positivity of cleaved caspase 3, and the lipid peroxidation, considered an index of intratumor oxidative stress, were low or undetectable in untreated and gemcitabine-treated animals, as well as in animals treated with low dosages of **FA4**, but they became more pronounced in tumors from animals treated with high dosages of **FA4** (Figure 7C-D). No treatment-related deaths, weight loss or abnormalities in mouse behavior were observed during treatment. Blood cells count and hematochemical parameters (AST, ALT, LDH, CPK, creatinine) were measured and no significant differences were noted between **FA4** treated mice (at both the concentrations used) and when compared to the control group (Table S1, Supplementary Information).

Discussions

Multifunctional thiosemicarbazones that bind sigma receptors and chelate metals had provided promising results in pancreatic cancer models both *in vitro* and *in vivo*. Herein, a panel of human and murine adenocarcinoma pancreatic cells genotypically and phenotypically different [27] were selected since previous experiments have well shown how diverse pancreatic cancer cells differently respond to the chemotherapeutic agents. [4] In all the cell lines, the presence of the sigma-2 receptors was evaluated by flow cytometry analyses: the expression of sigma-2 receptor in the adenocarcinoma cells was from 2 to 3 –fold higher compared to the non-tumor epithelial cells. On the other hand, the sigma-1 receptor subtype was equally expressed in the human pancreatic cancer cells and in the non-tumor immortalized counterparts. The binding affinity of the novel thiosemicarbazone **FA4** for sigma-2 receptors was evaluated by the classical radioligand binding assay revealing a low nanomolar K_i value consistent with the K_i of the lead compound siramesine. Binding affinities of **FA4** were also measured by flow cytometry analyses in the pancreatic cancer cells in which **FA4** cytotoxic effect mechanisms were herein investigated, revealing similar low nanomolar IC_{50} values in all the cells (IC_{50} values around 10 nM). Because **FA4** structure mimics siramesine's, we also measured binding affinity of **FA4** for sigma-1 receptor, as in our hands siramesine binds the two sigma subtypes equally well. [8] Despite the fact that a 5-fold lower affinity of **FA4** for sigma-1 receptor compared to the sigma-2 receptor was found (IC_{50} values around 50 nM), the sigma-1 receptor implication in the overall activity, although more marginal, cannot be ruled out.

Except for the murine PANC02 cells, **FA4** displayed a 3- to 8-fold more potent cytotoxic activity compared to the already known thiosemicarbazones (**MLP44**, **PS3** and **ACthio-1**) in all the adenocarcinoma cells investigated. Worthy of note is the activity of **FA4** in PANC-1, that is an aggressive cell line of clinical importance that eventually develops resistance to gemcitabine. [13] Indeed, while other sigma-2 'pure' ligands (devoid of metal chelation activity) [3] and the 'pure' metal chelator thiosemicarbazone **ACthio-1** (devoid of sigma-2 affinity) did not display cytotoxicity

in PANC-1 cells, the synergistic effect proper of the multifunctional agents seem to be a winning strategy in this cell line. Indeed, thiosemicarbazones carrying the sigma-receptor targeting basic moiety (**PS3**, **MLP44**, **FA4**) exert cytotoxicity in PANC-1 cells. In our hands, the best results were so far reached by the sigma-2 targeting thiosemicarbazones **MLP44** and **PS3**, but **FA4** performed better, with a more potent activity in PANC-1 cells and a lower cytotoxicity in non-tumor cells. Although HPDE cells are immortalized and do not exactly recapitulate the non-transformed epithelial pancreatic cells, this data gives an indication of a selective activity of **FA4** towards cancer cells rather than towards non-transformed cells. An important cytotoxic activity compared to the other thiosemicarbazones was also shown by **FA4** in the MiaPaCa2 cell line, another widely used pancreatic cancer model, although less aggressive and more sensitive to gemcitabine than PANC-1. [13]

The encouraging results from the cytotoxicity assays, that demonstrate a 'superior' activity of **FA4** in pancreatic cancer cells compared to the previously generated thiosemicarbazones, prompted us to analyze the possible apoptotic pathways induced by the four thiosemicarbazones (**FA4**, **MLP44**, **PS3** and **ACthio-1**) in our panel of diverse pancreatic adenocarcinoma cells. ER- dependent (ER stress sensors, caspase 7/caspase 3 axis) and mitochondria-dependent pathways (mitochondrial ROS and depolarization, caspase 9/caspase 3 axis) revealed variable activation of the apoptotic pathways dependent on ER and mitochondria, that depend on the cell line. The variegate results demonstrate that different pancreatic cells treated with the same compound undergo to cell death pathways to different extent and with different prevailing mechanisms. It is also clear as the modification of the basic moiety in these thiosemicarbazones leads to the activation of diverse pathways, dependent on ER or mitochondria. Noteworthy, **FA4** induces apoptosis and ER stress in all cell lines except for MiaPaCa2 cells, when used at its IC50 concentration that is in the low micromolar range. Although obtained *in vitro*, this result indicates a promising cytotoxic potential of **FA4** at concentrations that could be reached in preclinical models or even in clinical settings. The differential sensitivity of pancreatic cancer cell lines to **FA4** and other thiosemicarbazones may be due to several and

interconnected factors, including the reactivity of ER stress mechanisms, the vulnerability of mitochondria to the ROS-induced damage, the activity of autophagy.

Notably, while the other thiosemicarbazones have a variable effect on the activation of ER- or mitochondria-dependent pro-apoptotic axis, **FA4** activates both pro-apoptotic pathways in each cell line except for MiaPaCa2. The opposite behavior between MiaPaCa2 and the other cell lines indicates that the differences in the genotype and biochemical pathways of each cell line may widely affect the ability of slightly different thiosemicarbazones to drive or prevent pro-apoptotic pathways. At least two differences emerged between MiaPaCa2 and the other cell lines. First, in MiaPaCa2 cells **FA4** did not induce any increase in mitochondrial ROS that were the *primum movens* of the apoptosis induced by this thiosemicarbazone, according to the protective role of mitoQ. Second, we noticed different expression levels of authophagosome proteins and sequestration markers. This observation may have a relevant biological meaning because autophagy has been linked to the apoptotic mechanism activated by sigma-2 receptor. Importantly, pancreatic tumor cells less prone to undergo autophagic pathways are less responsive to therapy. [28] The results that autophagic proteins are less expressed in MiaPaCa2 cells compared to the other cell lines, suggest that MiaPaCa2 cells may be less reactive to cell death mechanisms induced by ER stress and mitochondrial damage elicited by **FA4**, due to a low autophagy. On the other hand, it is known that autophagy may play either a pro-tumor or an anti-tumor effect in pancreatic cancer [29]. Intriguingly, FA4 reduced the expression of specific autophagosome proteins and sequestration markers in all responsive cell lines, but not in MiaPaCa2 cells. We hypothesize that **FA4** prevents the protective/anti-tumor effect of autophagy in pancreatic cancer cells. By contrast, **FA4**-unresponsive MiaPaCa2 cells, which have a low and not tunable autophagy, are protected from **FA4**. These results suggest that the increase of mitochondrial ROS and/or the decrease in specific autophagic markers induced by FA4 are important in amplifying the cytotoxicity of **FA4** following ER stress and mitochondrial damage.

The promising cytotoxicity recorded *in vitro*, prompted to evaluate how **FA4** performed in xenografts *in vivo*. Our results showed that also the lower concentration of **FA4** was able to significantly reduce

tumor volume compared to control and gemcitabine. The effects observed in xenografts recapitulated the viability data observed *in vitro*. Indeed, **FA4** effectively reduced tumor growth of PANC-1 tumors, but not of MiaPaCa2 tumors. This result is of particular interest because PANC-1 xenografts were more resistant to gemcitabine than MiaPaCa2 xenografts. We recognize that we only compared one **FA4**-sensitive/gemcitabine resistant pancreatic tumor and one **FA4**-resistant/gemcitabine sensitive pancreatic tumor, but according to our data, we might speculate that **FA4** could be proposed as an alternative to gemcitabine in tumors unresponsive to the first line treatment. At short term, i.e. after 15 days of treatment, we could no detect a tumor regression in PANC-1 xenografts treated with **FA4**, but only a significant delay in tumor growth, followed by a cytostatic effect when animals were treated with the higher dosage of **FA4**. Since apoptosis dependent on ER stress and mitochondria depolarization is not the only mechanisms that can induce tumor regression, we may hypothesize that other driving factors, not affected by **FA4**, continue to stimulate tumor growth. Alternatively, we could not exclude that our treatment was too short to appreciate a pronounced apoptotic effect of **FA4**, able to determine tumor regression. To clarify this point and to deepen the safety profile of **FA4**, we doubled the time of treatment of PANC1 xenografts up to 30 days. In these conditions, the efficacy of **FA4** was amplified: indeed, the low dosage produced a cytostatic effect, while the high dose induced a tumor regression, likely due to the strong intratumor apoptosis. These data suggest that **FA4** is a well-tunable agent, able to exert either cytostatic or cytoreductive effects depending of the time and dosage chosen. Importantly, no signs of toxicity were recorded during and after treatment. Notably, in xenograft experiments, we used two concentrations (750 nM and 1.5 µM) that were below the IC50 of **FA4** (3.01 µM) in PANC1 cells. When used at the same concentration of its IC50, **FA4** activated the key mechanism related to its cytotoxic effect, i.e. the ER stress-dependent and the mitochondrial damage-dependent apoptosis in PANC1 cells. **FA4**-treated tumors recapitulated these events, as suggested by the increased intratumor active caspase 3 and by the increased lipid peroxidation, indicative of oxidative damage. These data suggest that the cytotoxic mechanisms observed *in vitro* also occur intratumorally.

In conclusion, through the use of metal chelator thiosemicarbazones targeting sigma receptors, (**FA4**, **MLP44**, and **PS3**) and **ACthio-1** (metal chelator), we have shown how small differences (i.e. diverse basic moiety) in the structure of thiosemicarbazone congeners lead to the activation of different pathways in the same cell types. Importantly, diverse cells undergo different pathways when treated with the same compound. These differences should be taken into account in the perspective of a personalized medicine based approach with therapies that can more efficiently target the peculiar characteristics of each tumor type. Additionally, the presence of the sigma-2 receptor targeting moiety may result in a more specific tumor delivery, given the higher density of these receptors in pancreatic tumors. Last but not the least, **FA4** provided promising antitumor activity in the aggressive PANC-1 preclinical tumor model, that is resistant to gemcitabine and is a prototypical example of pancreatic cancer that urgently needs novel treatment options. Our work highlights the potential of **FA4** as possible monotherapy against PDAC unresponsive to gemcitabine, as an alternative to the pharmaceutical strategies currently in use. Altogether, the results obtained encourage further studies to define **FA4** profile in patient-derived pancreatic adenocarcinomas, particularly for those tumors that, like PANC-1, are unresponsive to the conventional chemotherapy.

Materials and Methods

Biological Reagents

[^{3}H]-DTG (29 Ci/mmol) was purchased from PerkinElmer Life Sciences (Zavantem, Belgium). DTG was purchased from Tocris Cookson Ltd., U.K. (+)-Pentazocine was obtained from Sigma-Aldrich-RBI s.r.l. (Milan, Italy). Wistar Hannover rats (250-300 g) was from Harlan, Italy. Cell culture reagents were purchased from EuroClone (Milan, Italy). MTT (3-[4,5-dimethylthiazol-2-yl]-2,5-diphenyltetrazoliumbromide), was obtained from Sigma-Aldrich (Milan, Italy). [10-(2,5-dihydroxy-3,4-dimethoxy-6,ethylphenyl)decyl]triphenyl-phosphonium, monomethanesulfonate (mitoquinol or mitoQ) was from Cayman Chemical (Ann Arbor, MI).

Cell Culture

Human pancreas adenocarcinoma cancer cell lines BxPC3 (CRL-1687™), AspC1 (CRL-1682™), MiaPaCa2 (CRL-1420™), and PANC-1 (CRL-1469™) were obtained from American Type Culture Collection (ATCC®, Bethesda, MD). The murine PANC02 pancreas adenocarcinoma was a gift from Bryan Clary (Duke University). The KP02 mouse line was derived from pancreatic cancer tumor tissue obtained from p48-CRE/LSL-$Kras^{G12D}$/$p53^{flox/+}$ mice (backcrossed C57BL/6, n = 6). Non-tumor human pancreatic ductal epithelial (HPDE) cells were provided by Kerafast (cat. N° ECA001-FP, Boston, MA). AspC1, BxPC3 and PANC02 cells were cultured in RPMI-1640 medium with 10% fetal bovine serum (FBS). MiaPaCa2 cells were cultured in Dulbecco's Modified Eagle's Medium (DMEM) with 10% FBS and 2.5% horse serum. PANC-1 cells were cultured in DMEM with 10% FBS. KP02 cells were cultured in 1:1 mixture of DMEM and Ham's F-12 Nutrient Mixture with 10% FBS. HPDE were cultured in Keratinocyte/serum-free medium with EGF and bovine pituitary extract (Invitrogen). Penicillin (100 mg/mL) and streptomycin (100 mg/mL) were added to all media; cells were maintained in a humidified incubator at 37 °C with 5% CO_2.

Flow Cytometry studies

Flow cytometry studies to detect sigma receptors density and ligand binding affinity were carried out according to Abate et al 2016 [17] and Niso et al 2015 [15], for sigma-1 and sigma-2 receptor, respectively. In order to detect the sigma-2 receptor content in pancreatic cells together with the affinity of **FA4** for sigma-2 receptors in the same cells, MiaPaCa2, PANC-1 BxPC3, PANC02, KP02, AspC1 and HPDE cells were incubated with increasing concentrations (1, 10, and 100 nmol/L and 1 and 10 µM) of **FA4**, followed by 100 nmol/L of sigma-2 fluorescent compound (**NO1**, 2-{6-[2-(3-(6,7-dimethoxy-3,4-dihydroisoquinolin-2(1*H*)-yl)propyl)-3,4-dihydroisoquinolin-1(2*H*)-one-5-yloxy]hexyl}-5-(dimethylamino)isoindoline-1,3-dione) [15] for 75 min at 37 °C. To mask sigma-1 receptors, (+)-pentazocine (10 µM) was co-incubated. The same experiment was repeated with the sigma-2 reference compound DTG in place of **FA4**, as a validation procedure.

At the end of the incubation periods, cells were washed twice with PBS, detached with 200 mL of Cell Dissociation Solution (Sigma Chemical Co.) for 10 min at 37 °C, centrifuged at 13,000 g for 5 min and resuspended in 500 µL of PBS. The fluorescence was recorded using a Bio-Guava® easyCyte™ 5 Flow Cytometry System (Millipore, Billerica, MA), with a 530 nm band pass filter. For each analysis, 50,000 events were collected and analyzed with the InCyte software (Millipore).

Sigma-1 receptor density and **FA4** binding to sigma-1 receptors was measured in PANC-1, MiaPaCa2 and HPDE cells that were incubated with increasing concentrations (1, 10, and 100 nmol/L and 1 and 10 µM) of (+)-pentazocine or **FA4**, followed by 100 nmol/L of sigma-1 fluorescent compound (**LM1**, 5-(dimethylamino)-2-(6-((5-(4-(4-methylpiperidin-1-yl)butyl)-5,6,7,8-tetrahydronaphthalen-2-yl)oxy)hexyl)isoindoline-1,3-dione) [17] for 75 min at 37 °C. To mask sigma-2 receptors the sigma-2 receptor selective ligand **F390**, 2-(3-(6,7-dimethoxy-3,4-dihydroisoquinolin-2(1*H*)-yl)propyl)-5-methoxy-3,4-dihydroisoquinolin-1(2*H*)-one [18] (10 µM) was co-incubated. At the end of the incubation periods, cells were washed twice with PBS, detached with 200 mL of Cell Dissociation Solution (Sigma Chemical Co.) for 10 min at 37 °C, centrifuged at 13,000 g for 5 min and resuspended in 500 µL of PBS. The fluorescence was recorded using a Bio-Guava® easyCyte™ 5 Flow Cytometry System (Millipore, Billerica, MA), with a 530 nm band pass filter. For each analysis, 50,000 events were collected and analyzed with the InCyte software (Millipore).

Sigma-2 binding by radioligand studies

Sigma-2 receptor binding was carried out according to Berardi et al 2009. [30] [^{3}H]-DTG was used as sigma-2 receptor specific radioligand in the presence of 1 µM (+)-pentazocine to mask sigma-1 receptors, in rat liver membranes. DTG (85-96%) was used for the specific binding calculation. Concentrations required to inhibit 50% of radioligand specific binding (IC_{50}) were determined by using six to nine different concentrations of the drug studied in two or three experiments with samples in duplicate. Scatchard parameters (K_d and B_{max}) and apparent inhibition constants (K_i) values were determined by nonlinear curve fitting, using the Prism, version 5.0, GraphPad software (2009).

Cell Viability

Determination of cell growth was performed using the MTT assay at 48 h. [3,31] On day 1, 25,000 cells/well were seeded into 96-well plates in a volume of 100 μL. On day 2, the drugs at concentrations ranging from 1 μM to 100 μM were added. In all the experiments, the various drug-solvents (EtOH, DMSO) were added in each control to evaluate a possible solvent cytotoxicity. After the established incubation time with drugs (48 h), MTT (0.5 mg/mL) was added to each well, and after 3-4 h incubation at 37 °C, the supernatant was removed. The formazan crystals were solubilized using 100 μl of DMSO/EtOH (1:1) and the absorbance values at 570 and 630 nm were determined on the microplate reader Victor 3 from PerkinElmer Life Sciences.

Caspase 3, 7 and 9 activity

Caspase 3, caspase 7 and caspase 9 activation were measured by using the Caspase 3/7 Fluorescence Assay kit (Cayman Chemical, Ann Arbor, MI) and the Caspase 9 fluorimetric assay kit **(**Enzo Life Science, Roma, Italy). The results are expressed as nmol of the hydrolyzed substrate of each caspase/mg cellular proteins, according to a previously set titration curve.

qRT-PCR

Total RNA was extracted by phenol/chloroform method. 1 μg RNA was reverse-transcribed using the iScript Reverse Transcription Supermix kit (Bio-Rad Laboratories), according to the manufacturer's instruction. 25 ng cDNA were amplified with 10 μL IQ^{TM} SYBR Green Supermix (Bio-Rad Laboratories). Primers were designed with the qPrimer Depot software (http://primerdepot.nci.nih.gov/). qRT-PCR was carried out with a iQ^{TM}5 cycler (Bio-Rad Laboratories). Cycling conditions were: 30 s at 95°C, followed by 40 cycles of denaturation (15 s at 95°C), annealing/extension (30 s at 60°C). The same cDNA preparation was used to quantify the genes of interest and the housekeeping gene *S14*, used to normalize gene expression. The relative

quantitation of each sample was performed using the Gene Expression Quantitation software (Bio-Rad Laboratories). Results were expressed in arbitrary units. For each gene, the expression in untreated cells was considered "1".

Mitochondrial and total ROS measurement

Intramitochondrial ROS was measured using the fluorescent probe MitoSOX (Invitrogen), as per manufacturer's instruction. To measure total ROS, cells were incubated with the ROS–sensitive probe 5-(and-6)-chlorometyl-20,70-dichlorodihydro-fluorescein diacetate-acetoxymethyl ester (5 mmol/L; DCFDA-AM), as described by Riganti et al 2015. [32] The results are expressed as nmol/mg mitochondrial or cellular proteins, respectively.

Mitochondria depolarization

Staining with JC-1 fluorescent probe (Biotium Inc., Freemont, CA) was performed as detailed in Riganti et al 2015. [32] The fluorescence units were used to calculate the percentage of green-fluorescent (i.e., depolarized) mitochondria versus red-fluorescent (i.e., polarized) mitochondria.

Immunoblotting

Cells were rinsed with ice-cold lysis buffer (50 mM, Tris, 10 mM EDTA, 1% v/v Triton-X100), supplemented with the protease inhibitor cocktail set III (80 μM aprotinin, 5 mM bestatin, 1.5 mM leupeptin, 1 mM pepstatin; Calbiochem, San Diego, CA), 2 mM phenylmethylsulfonyl fluoride and 1 mM Na_3VO_4, then sonicated and centrifuged at 13,000 × g for 10 min at 4 °C. 20 μg protein extracts were subjected to SDS-PAGE and probed with the antibodies for: ATG5, ATG7, ATG12, beclin, p62, LC3, GRP78, ATF6, IRE-1α, PERK (all from Abcam, Cambridge, UK), followed by a peroxidase-conjugated secondary antibody (Bio-Rad Laboratories). The membranes were washed with Tris-buffered saline-Tween 0.1% v/v solution, and the proteins were detected by enhanced

chemiluminescence (Bio-Rad Laboratories). To check the equal control loading in lysates, samples were probed with an anti-β-tubulin (Santa Cruz Biotechnology Inc., Santa Cruz, CA) antibody.

Activities of pro-oxidant and anti-oxidant enzymes. The activity of NADPH oxidase was measured in cell lysates, by a chemiluminescence-based assay reported by Tassone et al, 2017 [33]. Results were expressed as RLU/mg cellular proteins. Superoxide dismutase and catalase actibities were measured with the colorimetric Superoxide Dismutase Activity Assay kit (Abcam) and with the Catalase Activity Assay kit (Abcam), as per manufacturer's instructions. Results were expressed as optical density (OD)/mg cellular proteins.

***In vivo* experiments**

2 x 10^5 PANC-1 or Mia-PaCa2 cells were inoculated subcutaneously in the right flank of 6-week old C57BL/6 female nude mice (Charles River Laboratories Italia, Calco), housed (5 per cage) under 12 h light/dark cycle, with food and drinking provided *ad libitum*. Tumor growth was measured daily by caliper, according to the equation (LxW^2)/2, where L=tumor length and W=tumor width. When tumors reached the volume of 100 mm^3, mice (n= 8/group) were randomized in the following groups and treated daily for 15 days or 30 days intraperitoneally as reported: 1) Vehicle group (100 µL saline solution); 2) $FA4^{low}$ group (750 nmol **FA4** in 100µL saline solution); 3) $FA4^{high}$ group (1500 nmol **FA4** in 100µL saline solution); 4) Gemcitabine group (20 mg/kg gemcitabine, twice a week). Tumor volumes and animals weight were monitored daily. Animals were euthanized at day 18 or 36 after randomization with zolazepam (0.2 ml/kg) and xylazine (16 mg/kg). Tumors were excised and paraffin-embedded. Sections were immuno-stained for cleaved caspase 3 (Cell Signalling technology, Danvers, MA) or with anti-malondialdehyde (Abcam) antibody, followed by a peroxidase-conjugated secondary antibody (Dako, Glostrup, Denmark). The sections were examined with a Leica DC100 microscope (Leica, Wetzlar, Germany). The quantitation of the immunohistochemical analyses was performed with the ImageJ software (https://imagej.nih.gov/). The staining intensity was expressed as arbitrary units and was considered 1 in vehicle group. Red blood cells (RBC) count, hemoglobin (Hb), white blood cells (WBC) count, platelets (PLT) count, lactate dehydrogenase (LDH), aspartate

aminotransferase (AST), alanine aminotransferase (ALT), alkaline phosphatase (AP), creatinine, creatine phosphokinase (CPK) were measured on blood samples collected immediately after euthanasia, using commercially available kits from Beckman Coulter Inc (Beckman Coulter, Miami, FL). In all studies, researchers analyzing the results were unaware of the treatments received by animals. The study complies with ARRIVE guidelines.

Statistical analysis

Unless specified, data plotting and statistical analysis were conducted using GraphPad Prism 5.0. Data were analyzed by applying the one-way repeated measures analysis of variance, and Bonferroni's multiple comparison test followed as a post hoc test. Results are reported as mean ± SEM (standard error of the mean) of at least two to three independent experiments, performed in triplicate. Statistical significance was accepted at $P < 0.05$.

Supplementary Information: Chemistry: experimental and Scheme S1; Hematochemical parameters of treated animals in Table S1; Density of sigma receptors in pancreatic cells by flow cytometry studies in Figure S1; Activation of caspase 3, 7, 9 in tumor pancreatic cells by **FA4** administered at its IC50 values in Figure S2; Immunoblot of GRP78, ATF6, IRE1 and PERK in tumor pancreatic cells treated with **FA4** at its IC50 values in Figure S3; NADPH oxidase, superoxide dismutase 1 and catalase, activities in tumor pancreatic cells treated with **FA4** in Figure S4; Growth of PANC-1 and MiaPaCa2 xenografts treated with **FA4**, in Figure S5.

Declaration Section

Partial financial support was received by Associazione Italiana per la Ricerca sul Cancro (AIRC grant: IG 21408).

The authors have no relevant financial or non-financial interests to disclose.

The authors have no conflicts of interest to declare that are relevant to the content of this article.

All authors certify that they have no affiliations with or involvement in any organization or entity with any financial interest or non-financial interest in the subject matter or materials discussed in this manuscript.

The authors have no financial or proprietary interests in any material discussed in this article.

Compliance with Ethical Standards

The animal care and experimental procedures were approved by the Bio-Ethical Committee of the Italian Ministry of Health (#122/2015-PR).

Authors' contribution

Carmen Abate, Chiara Riganti and Francesco Berardi designed and conceived the study. Material preparation and data collection were performed by Mauro Niso, Francesca Serena Abatematteo and Joanna Kopecka. Analyses of the data were performed by Carmen Abate and Chiara Riganti. The first draft of the manuscript was written by Carmen Abate and Chiara Riganti and all authors commented on previous versions of the manuscript. All authors read and approved the final manuscript.

References

1. R. L. Siegel, K. D. Miller, and A. Jemal, CA. Cancer J. Clin. **70**, 7 (2020).

2. M. L. Pati, M. Niso, S. Ferorelli, C. Abate, and F. Berardi, RSC Adv. **5**, 103131 (2015).

3. M. L. Pati, J. R. Hornick, M. Niso, F. Berardi, D. Spitzer, C. Abate, and W. Hawkins, BMC Cancer **17**, 1 (2017).

4. M. L. Pati, M. Niso, D. Spitzer, F. Berardi, M. Contino, C. Riganti, W. G. Hawkins, and C. Abate, Eur. J. Med. Chem. **144**, 359 (2018).

5. J. R. Hornick, S. Vangveravong, D. Spitzer, C. Abate, F. Berardi, P. Goedegebuure, R. H. MacH, and W. G. Hawkins, J. Exp. Clin. Cancer Res. **31**, 1 (2012).

6. J. R. Hornick, D. Spitzer, P. Goedegebuure, R. H. Mach, and W. G. Hawkins, Surgery **152**, S152 (2012).

7. Y. M. Hashim, D. Spitzer, S. Vangveravong, M. C. Hornick, G. Garg, J. R. Hornick, P. Goedegebuure, R. H. Mach, and W. G. Hawkins, Mol. Oncol. **8**, 956 (2014).

8. M. Niso, C. Abate, M. Contino, S. Ferorelli, A. Azzariti, R. Perrone, N. A. Colabufo, and F. Berardi, ChemMedChem **8**, 2026 (2013).

9. C. Abate, M. Niso, and F. Berardi, Future Med. Chem. **10**, 1997 (2018).

10. M. S. Ostenfeld, N. Fehrenbacher, M. Høyer-Hansen, C. Thomsen, T. Farkas, and M. Jäättelä, Cancer Res. **65**, 8975 (2005).

11. M. Hafner Ĉesen, U. Repnik, V. Turk, and B. Turk, Cell Death Dis. **4**, 1 (2013).

12. S. Ma, E. S. Henson, Y. Chen, and S. B. Gibson, Cell Death Dis. **7**, e2307 (2016).

13. F. Masetto, K. Chegaev, E. Gazzano, N. Mullappilly, B. Rolando, S. Arpicco, R. Fruttero, C. Riganti, and M. Donadelli, Biochim. Biophys. Acta. Mol. Cell Res. **1867**, 118824 (2020).

14. J. Perregaard, E. K. Moltzen, E. Meier, and C. Sánchez, J. Med. Chem. **38**, 1998 (1995).

15. M. Niso, C. Riganti, M. L. Pati, D. Ghigo, F. Berardi, and C. Abate, ChemBioChem **16**, 1078 (2015).

593 16. C. Cantonero, P. J. Camello, C. Abate, F. Berardi, G. M. Salido, J. A. Rosado, and P. C.
594 Redondo, Cancers (Basel). **12**, 1 (2020).
595 17. C. Abate, C. Riganti, M. L. Pati, D. Ghigo, F. Berardi, T. Mavlyutov, L.-W. Guo, and A.
596 Ruoho, Eur. J. Med. Chem. **108**, 577 (2016).
597 18. C. Abate, S. V Selivanova, A. Müller, S. D. Krämer, R. Schibli, R. Marottoli, R. Perrone, F.
598 Berardi, M. Niso, and S. M. Ametamey, Eur. J. Med. Chem. **69**, 920 (2013).
599 19. L. Longhitano, C. C. Castracani, D. Tibullo, R. Avola, M. Viola, G. Russo, O. Prezzavento, A.
600 Marrazzo, E. Amata, M. Reibaldi, A. Longo, A. Russo, N. L. Parrinello, and G. L. Volti,
601 Oncotarget **8**, 91099 (2017).
602 20. Y.-S. Huang, H.-L. Lu, L.-J. Zhang, and Z. Wu, Med. Res. Rev. **34**, 532 (2014).
603 21. A. Tesei, M. Cortesi, A. Zamagni, C. Arienti, S. Pignatta, M. Zanoni, M. Paolillo, D. Curti, M.
604 Rui, D. Rossi, and S. Collina, Front. Pharmacol. **9**, 1 (2018).
605 22. H. Terai, S. Kitajima, D. S. Potter, Y. Matsui, L. G. Quiceno, T. Chen, T.-J. Kim, M. Rusan, T.
606 C. Thai, F. Piccioni, K. A. Donovan, N. Kwiatkowski, K. Hinohara, G. Wei, N. S. Gray, E. S.
607 Fischer, K.-K. Wong, T. Shimamura, A. Letai, P. S. Hammerman, and D. A. Barbie, Cancer Res.
608 **78**, 1044 (2018).
609 23. R. H. Mach, C. Zeng, and W. G. Hawkins, J. Med. Chem. **56**, 7137 (2013).
610 24. C. Zeng, J. Rothfuss, J. Zhang, W. Chu, S. Vangveravong, Z. Tu, F. Pan, K. C. Chang, R.
611 Hotchkiss, and R. H. Mach, Br. J. Cancer **106**, 693 (2012).
612 25. J.-P. Decuypere, G. Monaco, G. Bultynck, L. Missiaen, H. De Smedt, and J. B. Parys, Biochim.
613 Biophys. Acta - Mol. Cell Res. **1813**, 1003 (2011).
614 26. T.-P. Su, T.-C. Su, Y. Nakamura, and S.-Y. Tsai, Trends Pharmacol. Sci. **37**, 262 (2016).
615 27. E. L. Deer, J. González-Hernández, J. D. Coursen, J. E. Shea, J. Ngatia, C. L. Scaife, M. A.
616 Firpo, and S. J. Mulvihill, Pancreas **39**, 425 (2010).
617 28. E. Giovannetti, Q. Wang, A. Avan, N. Funel, T. Lagerweij, J.-H. Lee, V. Caretti, A. van der
618 Velde, U. Boggi, Y. Wang, E. Vasile, G. J. Peters, T. Wurdinger, and G. Giaccone, J. Natl. Cancer

Inst. **106**, djt346 (2014).

29. V. E. Gómez, E. Giovannetti, and G. J. Peters, Semin. Cancer Biol. **35**, 11 (2015).

30. F. Berardi, C. Abate, S. Ferorelli, V. Uricchio, N. A. Colabufo, M. Niso, and R. Perrone, J. Med. Chem. **52**, 7817 (2009).

31. C. Riganti, R. Giampietro, J. Kopecka, C. Costamagna, F. S. Abatematteo, M. Contino, and C. Abate. Int. J. Mol. Sci. **21**, 3333 (2020).

32. C. Riganti, E. Gazzano, G. R. Gulino, M. Volante, D. Ghigo, and J. Kopecka, Cancer Lett. **360**, 219 (2015).

33. B. Tassone, S. Saoncella, F. Neri, U. Ala, D. Brusa, M. A. Magnuson, P. Provero, S. Oliviero, and C. Riganti, E. Calautti. Cell Death Differ. **24**, 731 (2017).

Table 1. Binding affinity values of **FA4** and reference compounds at sigma receptors.

	Binding Assay						
Cmpd	Radioligand, K_i ± SEM[a] (nM)	Flow Cytometry, IC_{50} ± SEM[a] (μM)					
	Sigma-2	*Sigma-2*				*Sigma-1*	
	Rat Liver	**MiaPaCa2**	**PANC-1**	**AspC1**	**KP02**	**MiaPaCa2**	**PANC-1**
FA4	15.8 ±3.6	9.13±1.1	11.4±2.3	10.6±2.2	11.6±1.5	53.2±5.6	51.3±4.3
DTG	22.5±3.6	5.98±0.9	6.59±1.6	14.3±3.0	7.16±1.2		
(+)-pentazocine						12.8±2.1	29.3±3.9

[a] Values represent the mean of n ≥ 3 separate experiments in duplicate ± SEM.

Table 2. Activity values of thiosemicarbazones compounds in pancreatic cell lines.

Cmpd	**Activity in pancreatic cell lines, EC_{50} ± SEM[a] (μM)**						
	Tumor cells						**Normal cells**
	MiaPaCa2	**PANC-1**	**AspC1**	**BxPC3**	**KP02**	**PANC02**	**HPDE**
FA4	1.98±0.4	3.01±0.8	1.39±0.3	1.36±0.2	0.88±0.1	1.94±0.5	6.11±1.1
MLP44[b]	14.6	14.6	2.01	2.34	6.92	1.33	9.50
PS3[b]	10.08	8.73	3.86	6.15	7.32	1.17	5.35
Acthio1[b]	18.3	>100	2.17	2.52	2.83	1.21	10.5

[a] Values represent the mean of n ≥ 3 separate experiments in duplicate ± SEM; [b] From ref [4]

638 **Figure 1.** Known (**AcThio-1**, **PS3** and **MLP44**) and novel (**FA4**) thiosemicarbazones.

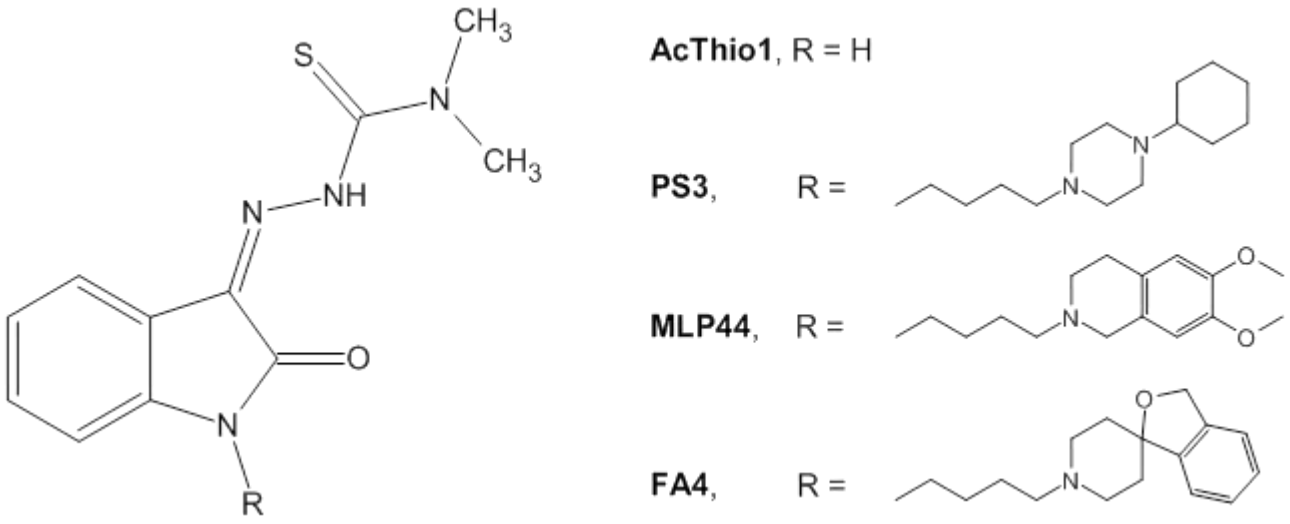

639

Figure 2. Activation of caspase 3, 7, 9 by thiosemicarbazones in pancreatic cell lines. Fluorimetric measure of caspase 3, 7, 9 in cells treated 2 h with 50 µM of each compounds. Results are means ± SEM (n = 3), $P < 0.05$.

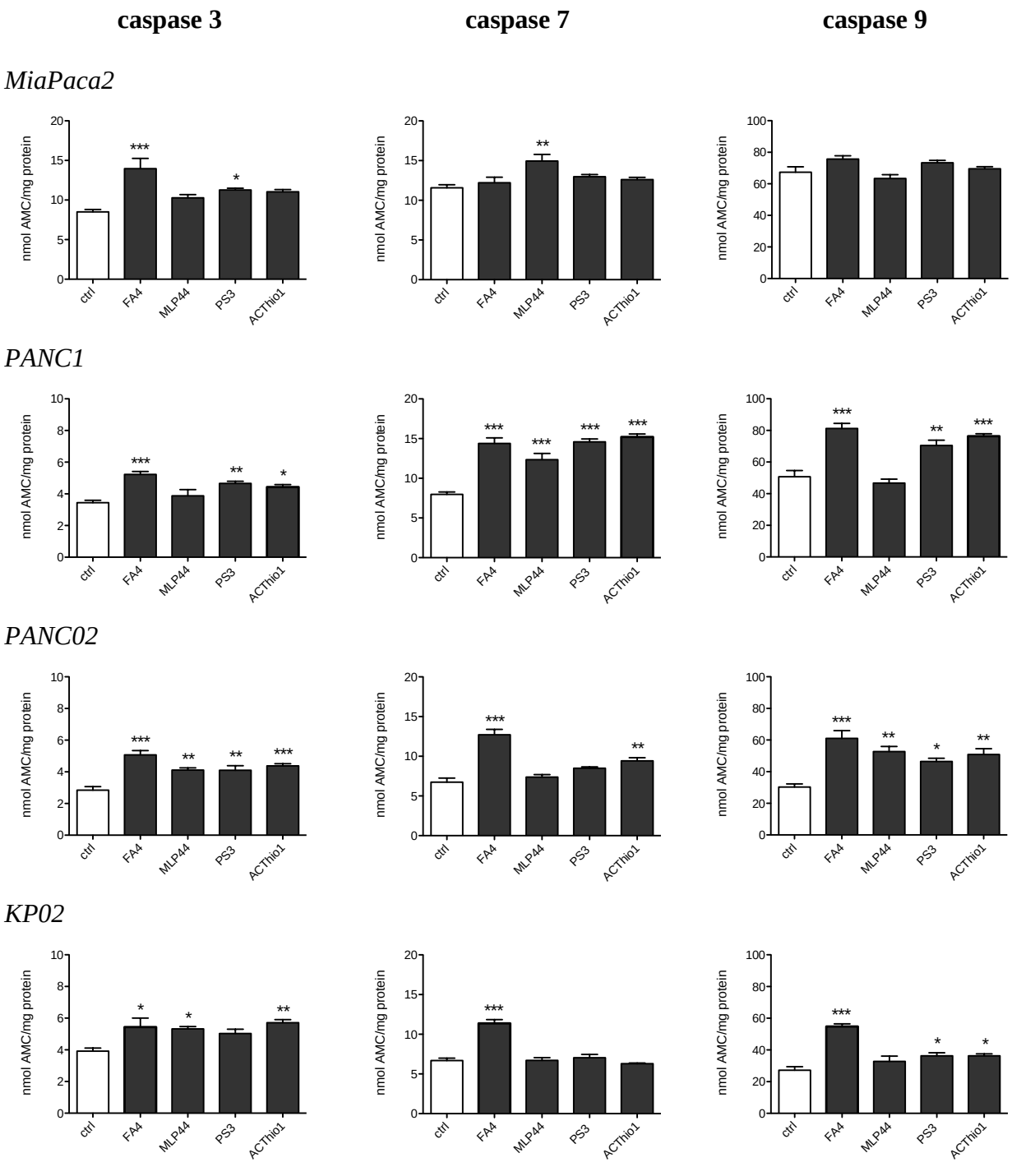

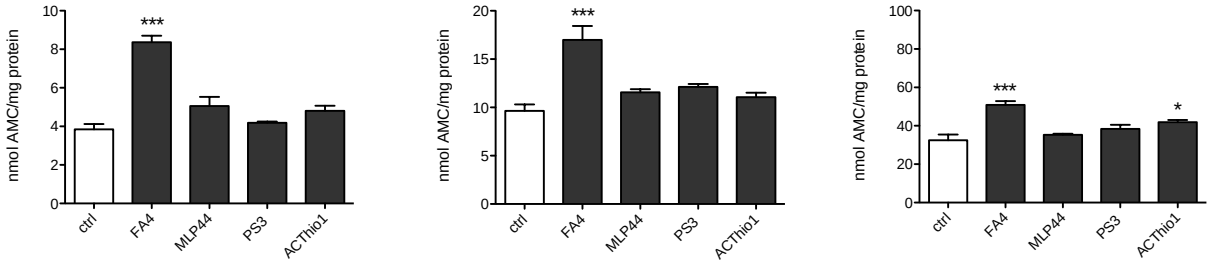
nmol AMC/mg protein
10
8
6
4
2
0
***
ctrl
FA4
MLP44
PS3
ACThio1
nmol AMC/mg protein
20
15
10
5
0
***
ctrl
FA4
MLP44
PS3
ACThio1
nmol AMC/mg protein
100
80
60
40
20
0
***
*
ctrl
FA4
MLP44
PS3
ACThio1

643

644

645

Figure 3. ER markers in thiosemicarbazone-treated pancreatic cancer cells. **A.** mRNA expression of ER stress markers, measured by RT-PCR, in cells treated 2 h with 50 µM of each compounds. Results are means ± SEM (n = 3), $P < 0.05$. **B.** Immunoblot of GRP78, ATF6, IRE1 and PERK in the indicated cell lines incubated with FA4 at 50 µM for 2 h. The image is representative of three independent experiments. Tubulin was used as control of equal protein loading.

A

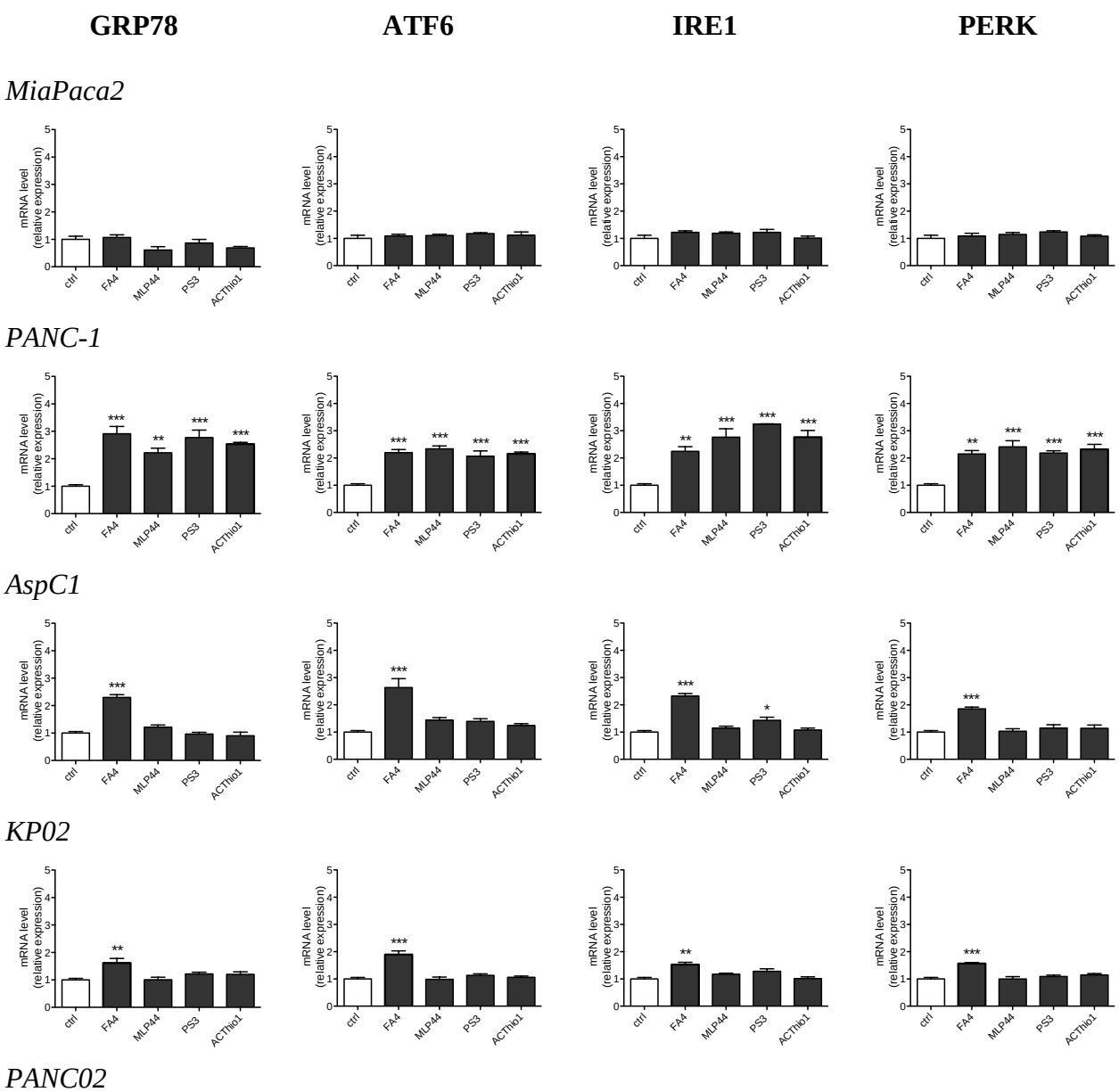

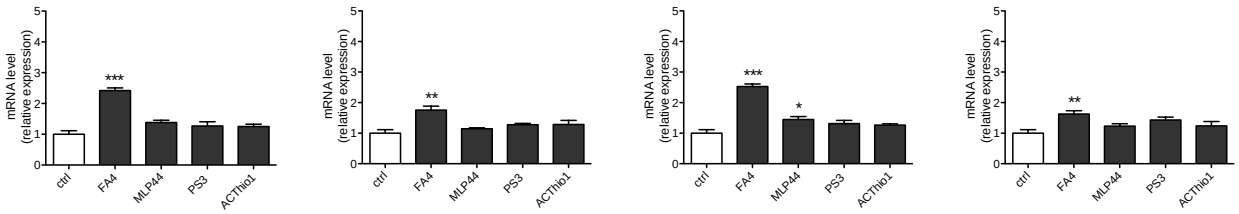
mRNA level
(relative expression)
ctrl
FA4
MLP44
PS3
ACThio1

B

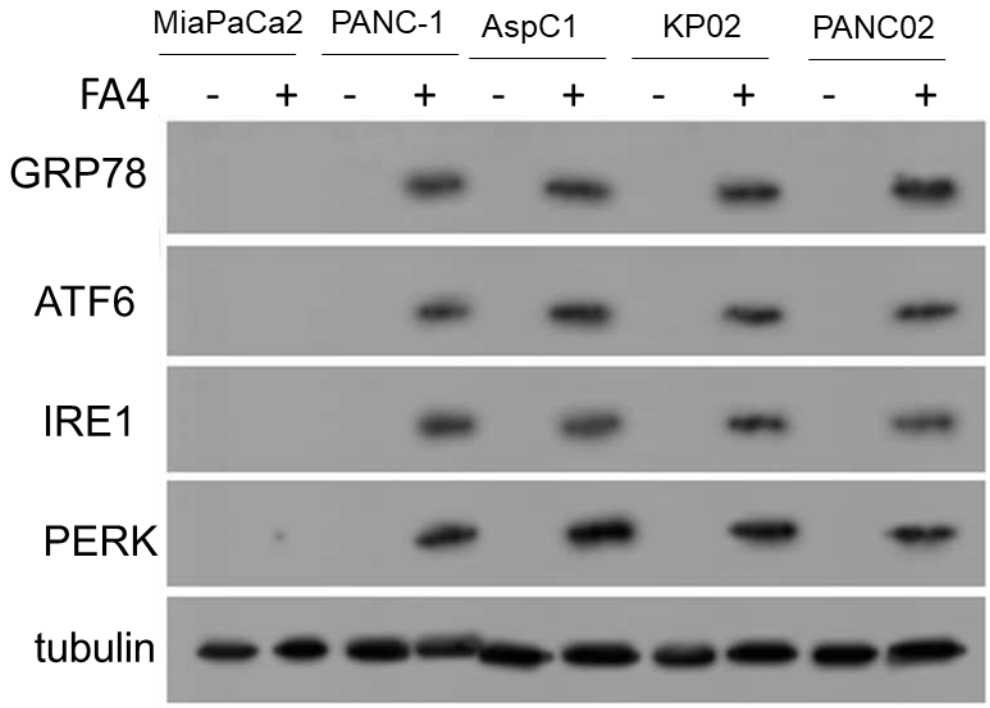
MiaPaCa2
PANC-1
AspC1
KP02
PANC02
FA4
GRP78
ATF6
IRE1
PERK
tubulin

Figure 4. ROS and mithocondrial damage markers in thiosemicarbazones-treated pancreatic cell lines. Fluorimetric staining of mitochondrial ROS (MitoSOX staining, **A**), whole cell ROS (DCFDA-AM probe, **B**) and mitochondria depolarization (JC1 staining, **C**) in cells treated 2 h with 50 µM of each compounds. Results are means ± SEM (n = 3), $P < 0.05$.

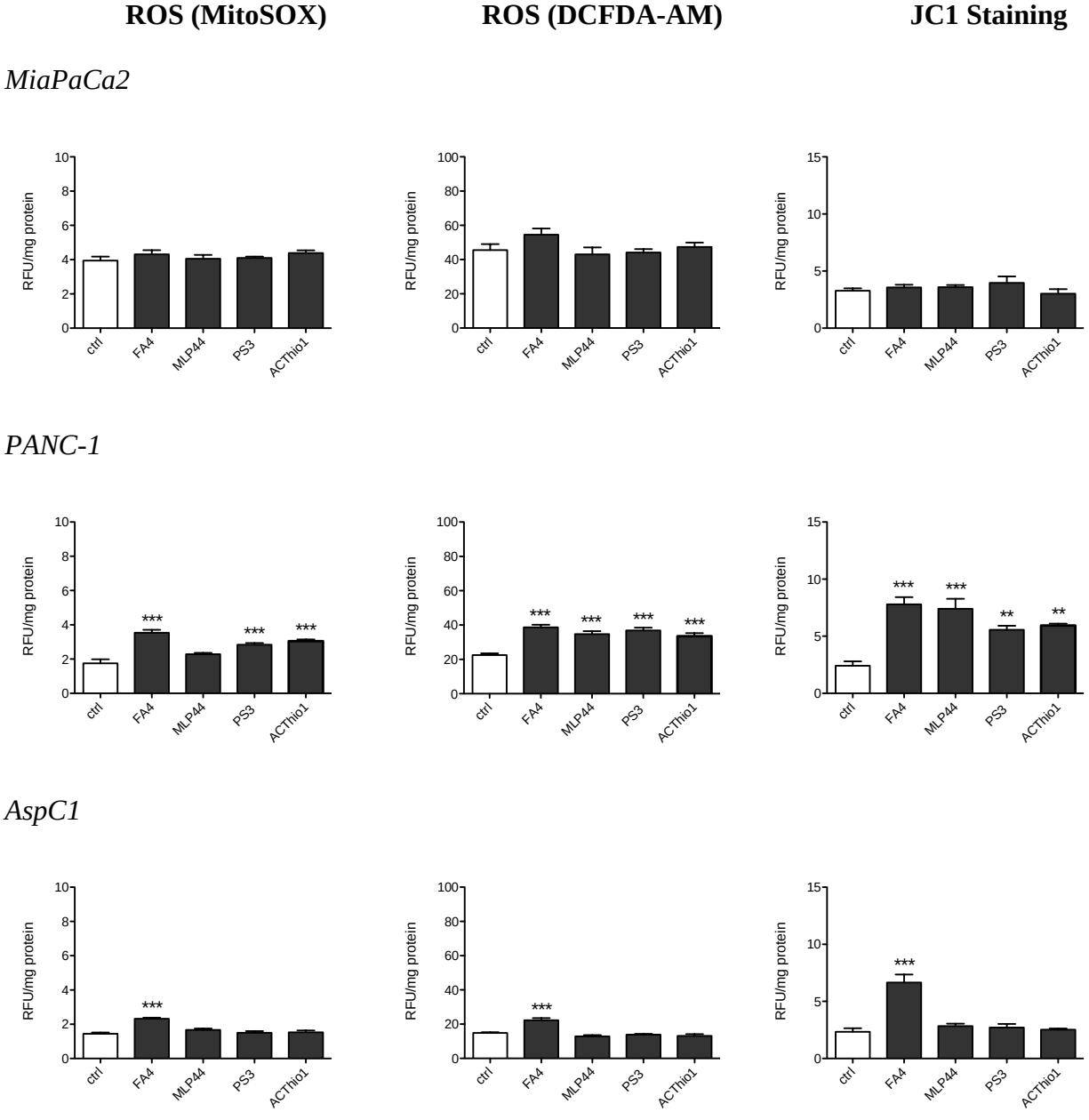

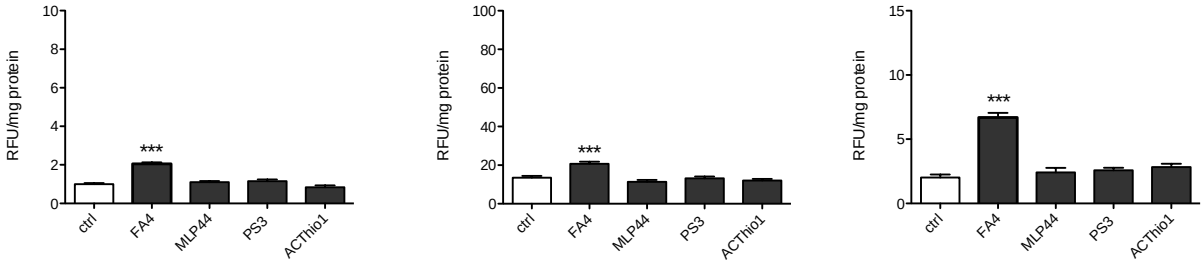

PANC02

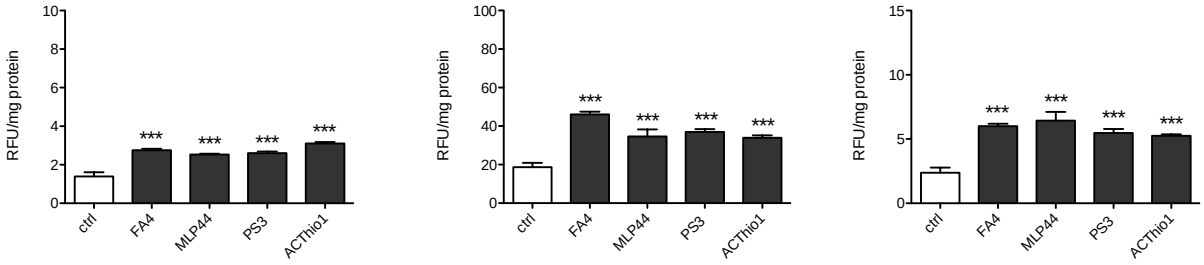

667

668

669 **Figure 5.** Mitochondrial ROS (**A**), activation of caspase 9 (**B**) and caspase 3 (**C**) in cells treated 2 h

670 with 50 µM of **FA4** alone or plus 0.4 µM mitoquinol, chosen as scavenger of mitochondrial ROS.

671 Results are means ± SEM (n = 3), $P < 0.05$.

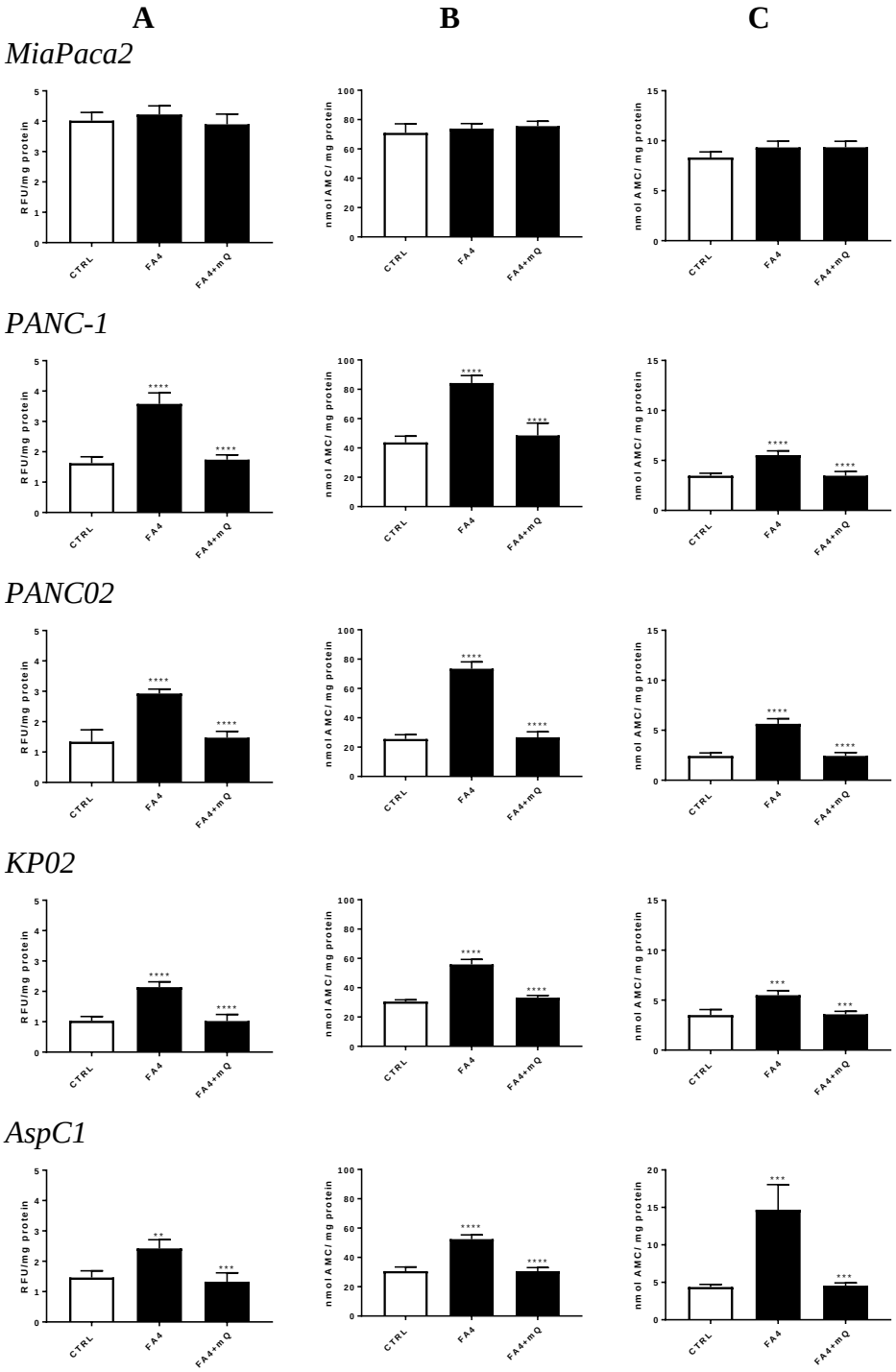

672

Figure 6. Markers of authophagy and protein sequestration in pancreatic cell lines. Immunoblot of the indicated proteins in cells treated 2 h with 50 μM of **FA4**. The image is representative of three independent experiments. Tubulin was used as control of equal protein loading.

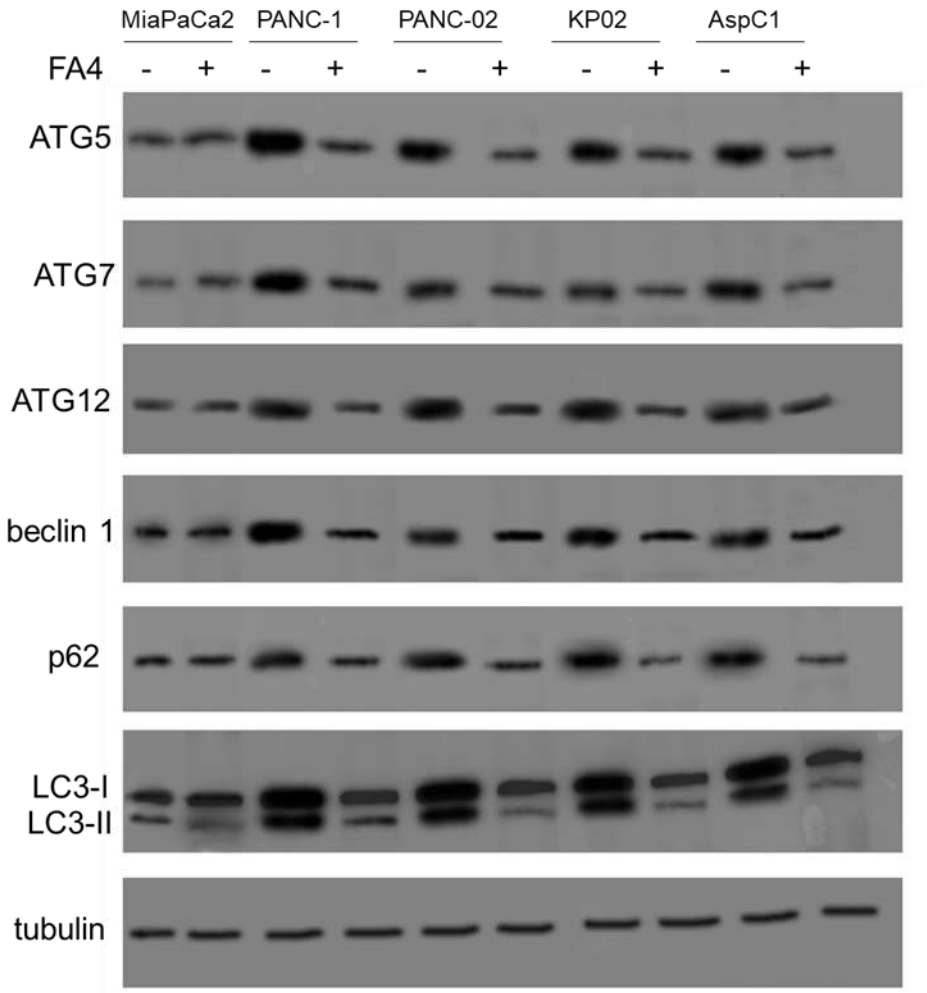

Figure 7. FA4 in C57BL/6 mice bearing PANC-1 tumors, treated for 30 days. 1) Vehicle group (black line, 100 µL saline solution); 2) FA4^{low} group (red line, 750 nmoles FA4 in 100 µL saline solution); 3) FA4^{high} group (yellow line, 1500 nmoles FA4 in 100 µL saline solution); 4) Gemcitabine group (green line, 20 mg/kg gemcitabine, twice a week). Animals were euthanized at day 36. **A.** Tumor growth. Results are means ± SEM (n = 8). ***P<0.001: FA4-groups *vs* vehicle (days 21-36); $^{\#\#}$P<0.001: FA4-groups *vs* gemcitabine (days 21-36); °°°P<0.001: FA4^{high}-group vs FA4^{low}-group (days 21-36). **B.** Representative photos of excised tumors. **C.** Immunohistochemical analysis of intratumor cleaved caspase 3 and malondialdehyde, as index of lipid peroxidation. The images are representative of each group of treatment. Ocular: 10X; objective: 20X. Bars: 50 µm. **D.** The quantitation of the immunohistochemical staining were performed with the Image J software. Results are means ± SEM (n = 8). ***P<0.001: FA4-groups *vs* vehicle; $^{\#\#}$P<0.01, $^{\#\#\#}$P<0.001: FA4-groups *vs* gemcitabine.

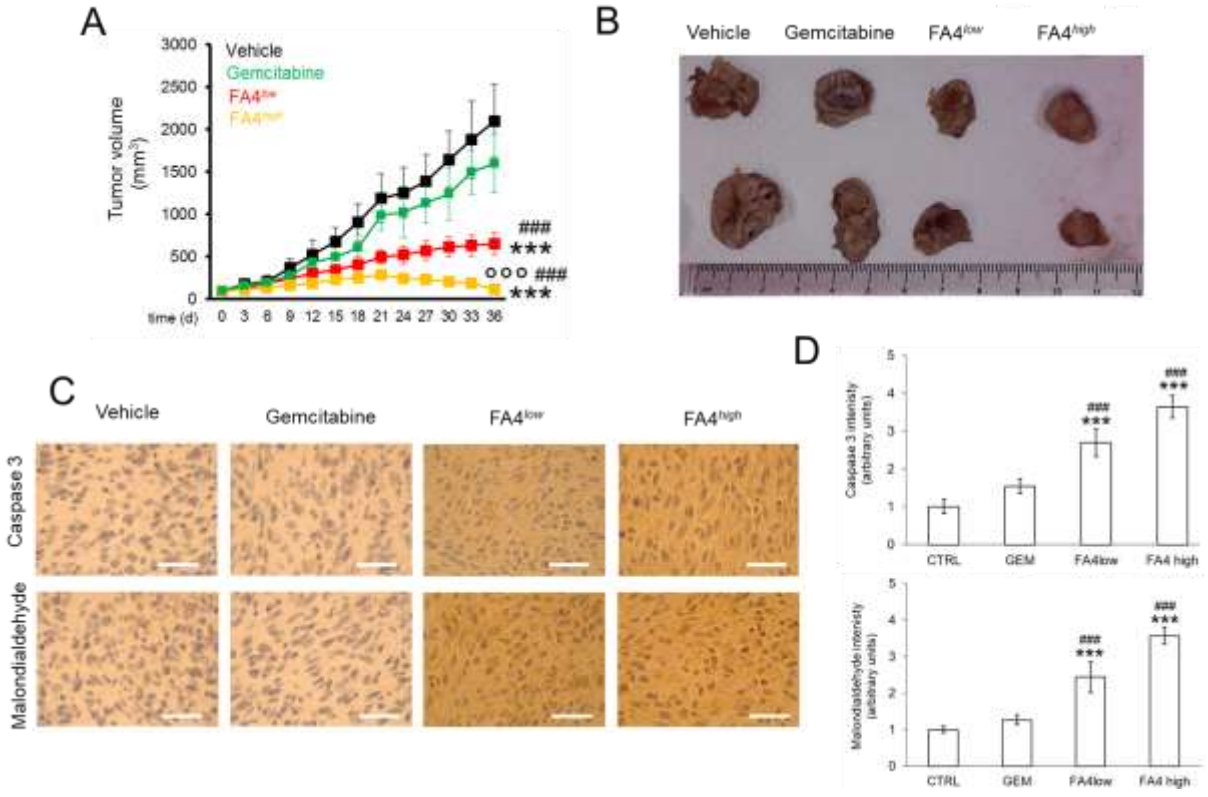

Supplementary Information

Multifunctional thiosemicarbazones targeting sigma receptors: *in vitro* and *in vivo* antitumor activity in adenocarcinoma pancreatic models

Mauro Niso[a#], Joanna Kopecka[b#], Francesca Serena Abatematteo[a], , Francesco Berardi [a], Chiara Riganti[b*], Carmen Abate[a*]

[a]Università degli Studi di Bari ALDO MORO, Dipartimento di Farmacia-Scienze del Farmaco, Via Orabona 4, 70125 Bari.
[b]Department of Oncology, University of Turin, via Santena 5/bis, 10126, Torino, Italy

[#]Equally Contributing Authors

[*]Corresponding Authors
Chiara Riganti, via Santena 5/bis, 10126, Torino, Italy, +390116705857, chiara.riganti@unito.it
Carmen Abate, via Orabona 4, 70125, Bari, Italy, +390805442231, carmen.abate@uniba.it

Table of Contents (total of 6 pages)

Chemistry

Column chromatography was performed with 60 Å pore size silica gel as the stationary phase (1:30 w/w, 63−200 μm particle size, from ICN). Melting points was determined in open capillaries on a Gallenkamp electrothermal apparatus. Purity of **FA4** was established by high-performance liquid chromatography (HPLC) on an Agilent Infinity 1260 system equipped with diode array with a multiwavelenght UV/vis detector set at λ = 230 nm, 254 nm and 280 nm, through a Phenomenex Gemini RP-18 column (250 × 4.6 mm, 5 μm particle size, MeOH/H_2O, 80:20 v/v at a flow rate of 0.8 mL/min). ^1H NMR spectra were recorded on a 500-vnmrs500 Agilent spectrometer (499.801 MHz). The following data were reported: chemical shift (δ) in parts per million (ppm), multiplicity (s = singlet, d = doublet, t = triplet, m = multiplet), integration, and coupling constant(s) in hertz. Mass spectrum was recorded on an Agilent 6890-5973 MSD gas chromatograph/mass spectrometer. High resolution mass spectroscopy (HRMS) was performed on a Agilent 6530 Accurate-Mass Q-TOF LC/MS spectrometer. Chemicals were from Aldrich, and were used without any further purification.

1-[4-(3*H*-spiro[isobenzofuran-1,4'-piperidine]-1'-yl)butyl]indoline-2,3-dione. (2)

A solution of **1** (0.297 g, 1.25 mmol) in CH_3CN (10 mL) was added with K_2CO_3 (0.143 g, 1.04 mmol) and 3*H*-spiro[isobenzofuran-1,4'-piperidine (0.196 g, 1.04 mmol). The resulting mixture was stirred under reflux overnight. The solvent was then removed under reduced pressure, and the residue was taken up with H_2O and extracted with CH_2Cl_2 (3 × 7 mL). The collected organic layers were dried (Na_2SO_4) and evaporated under reduced pressure to afford a crude dark-red oil which was purified by column chromatography (AcOEt/MeOH 9:1) to give the title compound. GC/MS *m*/*z* 390 (M^+, 10), 362 (15), 202 (100). The free base, dissolved in CH_2Cl_2 was transformed into the corresponding hydrochloride salt by addition of a solution of Et_2O saturated with gaseous HCl. QTOF-HRMS for $C_{24}H_{26}N_2O_3$ (*m*/*z*): $[M+H]^+$ calcd, 391.2022; found, 391.2021; $[M+Na]^+$ calcd, 413.1841; found, 413.1832.

(*Z*)-2-(1-(4-(3*H*-spiro[isobenzofuran-1,4'-piperidine]-1'-yl)butyl)-2-oxoindolin-3-ylidene)-*N*,*N*-dimethylhydrazinecarbothioamide hydrochloride. (FA4) 4,4-Dimethyl-3-thiosemicarbazide (0.017 g, 0.14 mmol) was added to a solution of **2** (0.055 g, 0.13 mmol) in hot ethanol and the mixture was refluxed for 5h. Upon cooling, a solid was obtained, filtered and washed with cold EtOH. Crystallization from EtOH (absolute) provided the title compound as yellow crystals (0.048 g, 70% yield), mp = 203-204 °C; ^{1}H NMR (500 MHz, CD_3OD) δ 1.80-1.90 (m, 4H), 1.92-1.98 (m, 2H), 2.25-2.35 (m, 2H), 3.15-3.25 (m, 2H), 3.40 (m, 4H), 3.48 (s, 6H), 3.93 (t, 2H, J = 6.4 Hz), 5.10 (s, 2H), 7.14-7.22 (m, 3H), 7.27-7.36 (m, 3H), 7.43 (dt, 1H, J_1 = 7.8 Hz, J_2 = 1.5 Hz), 7.88 (br s, 1H, NH), 7.90-7.93 (m, 1H), 8.42 (s, 1H); QTOF-HRMS for $C_{24}H_{26}N_2O_3$ (*m*/*z*): $[M+H]^+$ calcd, 492.2433; found, 492.2434.

Scheme S1

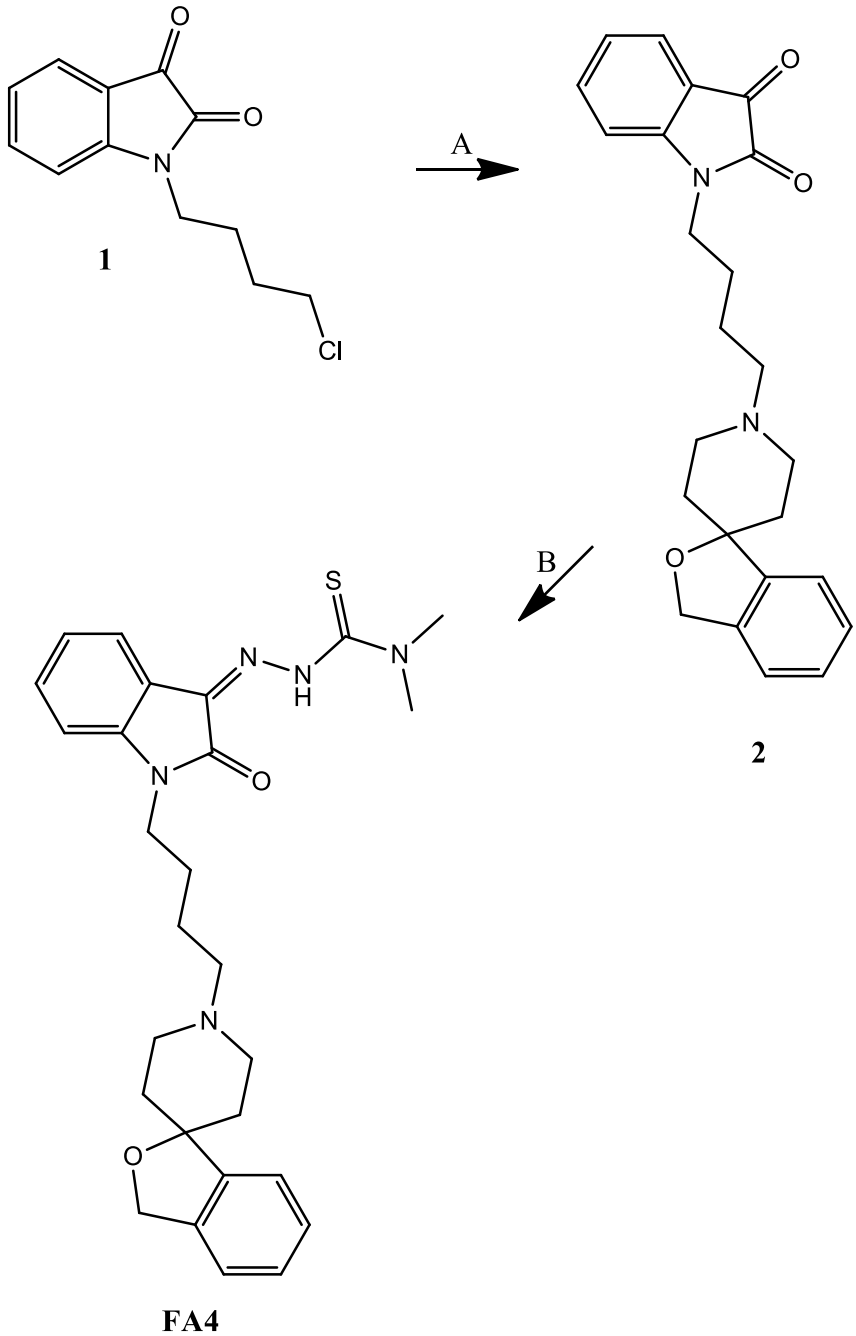

1 **2** **FA4**

Reagents: A) 3*H*-spiro[isobenzofuran-1,4'-piperidine, K_2CO_3, CH_3CN, Δ; B) 4,4-Dimethyl-3-thiosemicarbazide, EtOH, Δ.

Table S1. Hematochemical parameters of treated animals

	Ctrl	FA4 *low*	FA4 *high*	GEM
RBC (x 10^6/µl)	14.09±1.937	12.67±2.39	13.26 ±2.37	11.28±0.98
Hb (g/dl)	13.98±1.18	12.87±3.43	12.83.2-83	11.03±1.94
WBC (x 10^3/µl)	15.69±3.48	14.38±3.95	16.07±3.59	12.18±2.39
PLT (x 10^3/µl)	984±302	983±283	1192±334	931±165
LDH (U/l)	6594±1294	6453±604	7539±506	6704±832
AST (U/l)	103±29	132±48	115±29	142±18
ALT (U/l)	39±10	35±7	38±11	36±12
AP (U/l)	107±14	117±32	162±45	134±43
Creatinine (mg/l)	0.078±0.014	0.084±0.009	0.075±0.010	0.084±0.008
CPK (U/l)	384±44	376±81	309±34	309±32

Mice were treated as described in Figure 6. Blood was collected immediately after euthanasia and analyzed for red blood cells (RBC) count, hemoglobin (Hb), white blood cells (WBC) count, platelets (PLT) count, lactate dehydrogenase (LDH), aspartate aminotransferase (AST), alanine aminotransferase (ALT), alkaline phosphatase (AP), creatinine, creatine phosphokinase (CPK). Data are presented as means ± SD.

Figure S1. Density of sigma receptors in pancreatic cells by flow cytometry studies. Results are means ± SEM (n = 3), $P < 0.05$.

A. Density of sigma-2 receptor in pancreatic cells

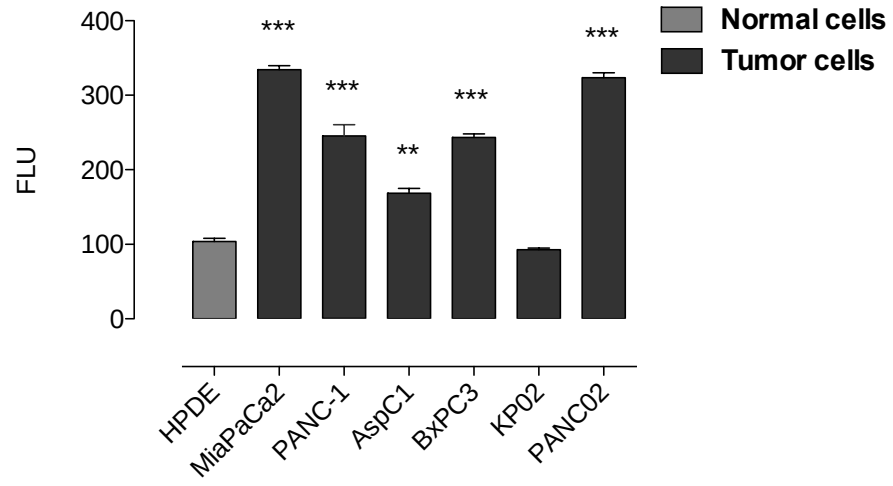

B. Density of sigma-1 receptor in pancreatic cells

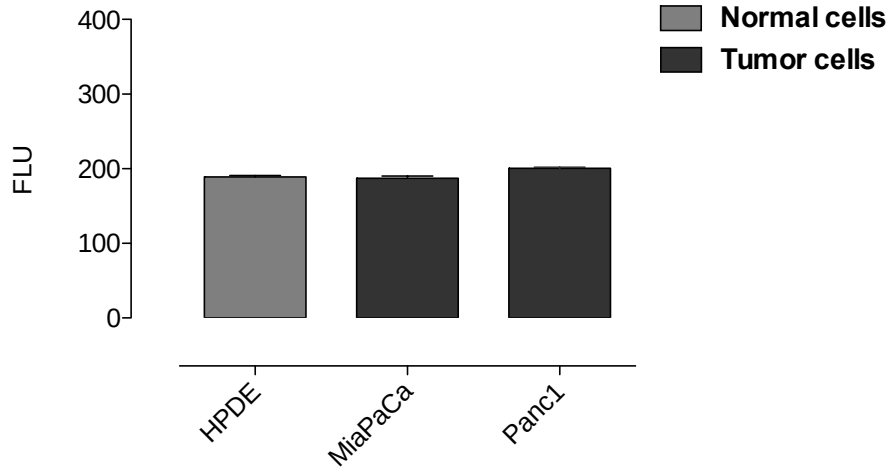

Figure S2. Activation of caspase 3, 7, 9 by **FA4** in pancreatic cell lines. Fluorimetric measure of caspase 3, 7, 9 in cells treated 2 h with a concentration of **FA4** corresponding to its IC50 in each cell line (see Table 2). Results are means ± SEM (n = 3), $P < 0.05$.

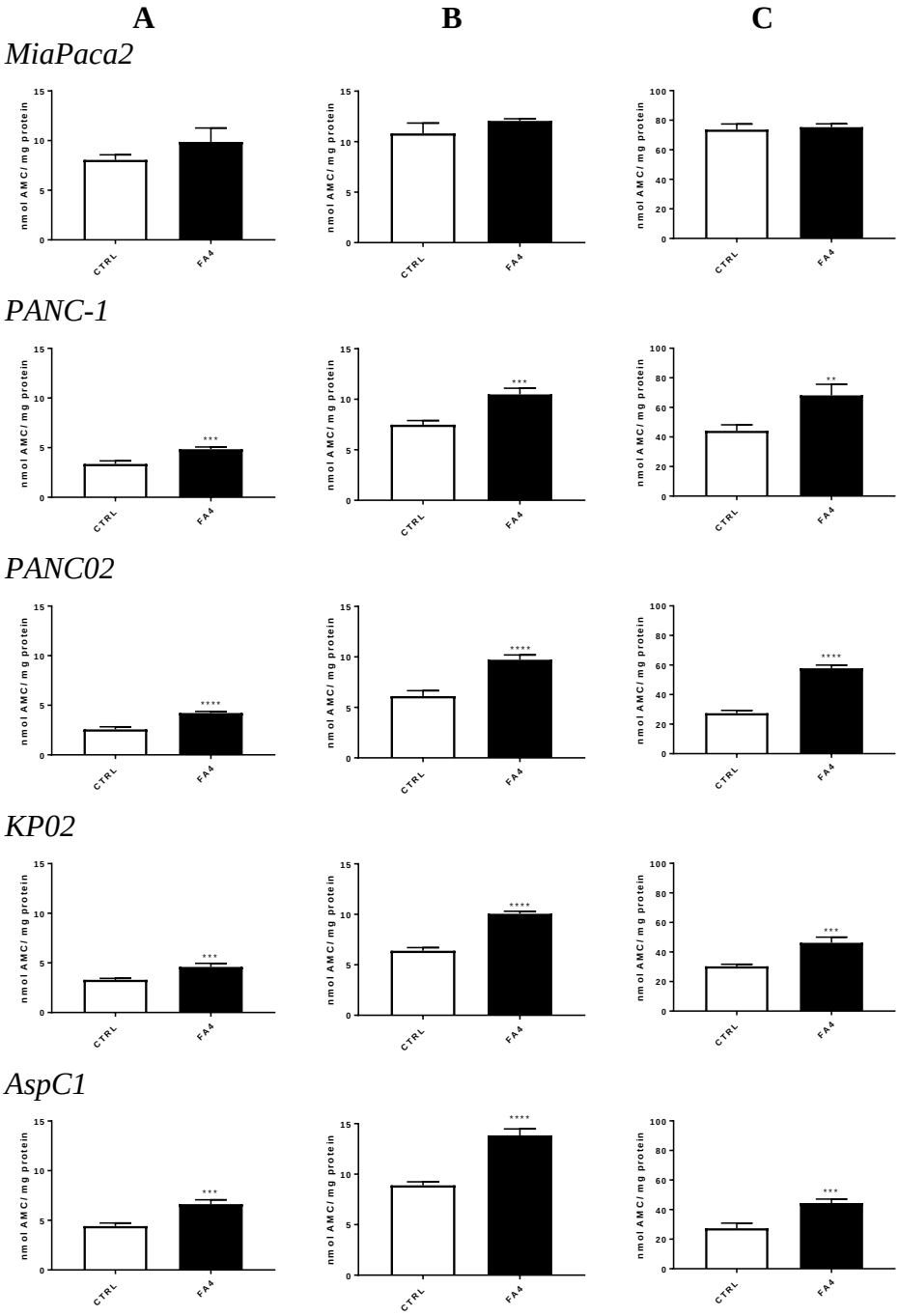

Figure S3. Immunoblot of GRP78, ATF6, IRE1 and PERK in the indicated cell lines treated 2 h with a concentration of **FA4** corresponding to its IC50 in each cell line (see Table 2). The image is representative of three independent experiments. Tubulin was used as control of equal protein loading.

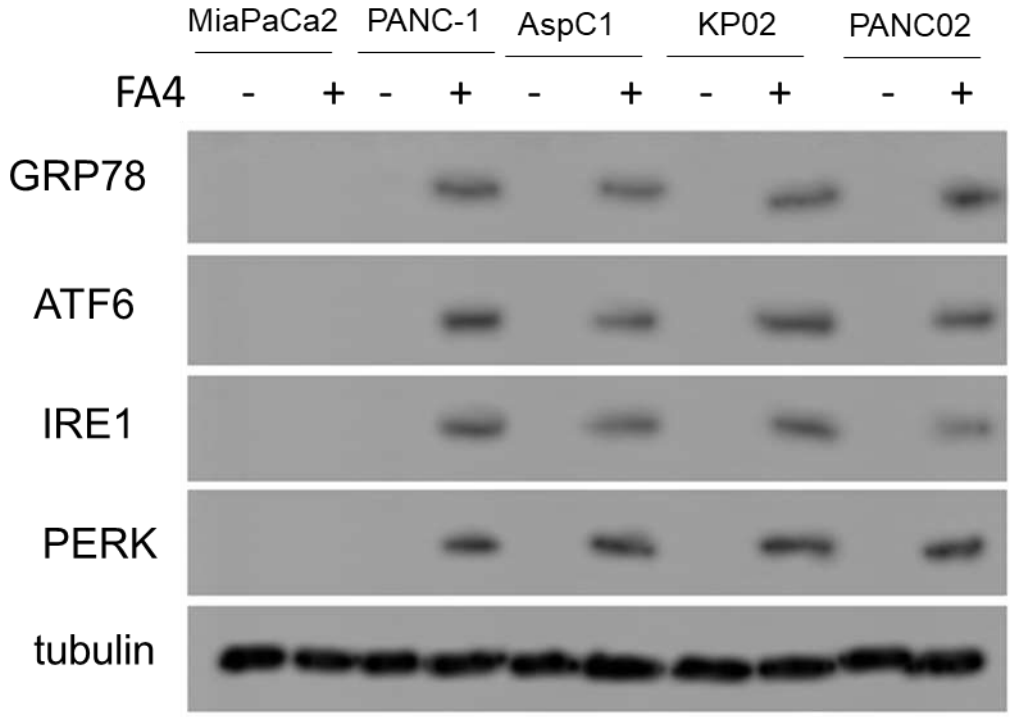

Figure S4. Activities of pro-oxidant NADPH oxidase (A) and anti-oxidant superoxide dismutase 1 (B), and catalase (C) enzymes in cells treated treated 2 h with 50 µM **FA4**. Results are means ± SEM (n = 3).

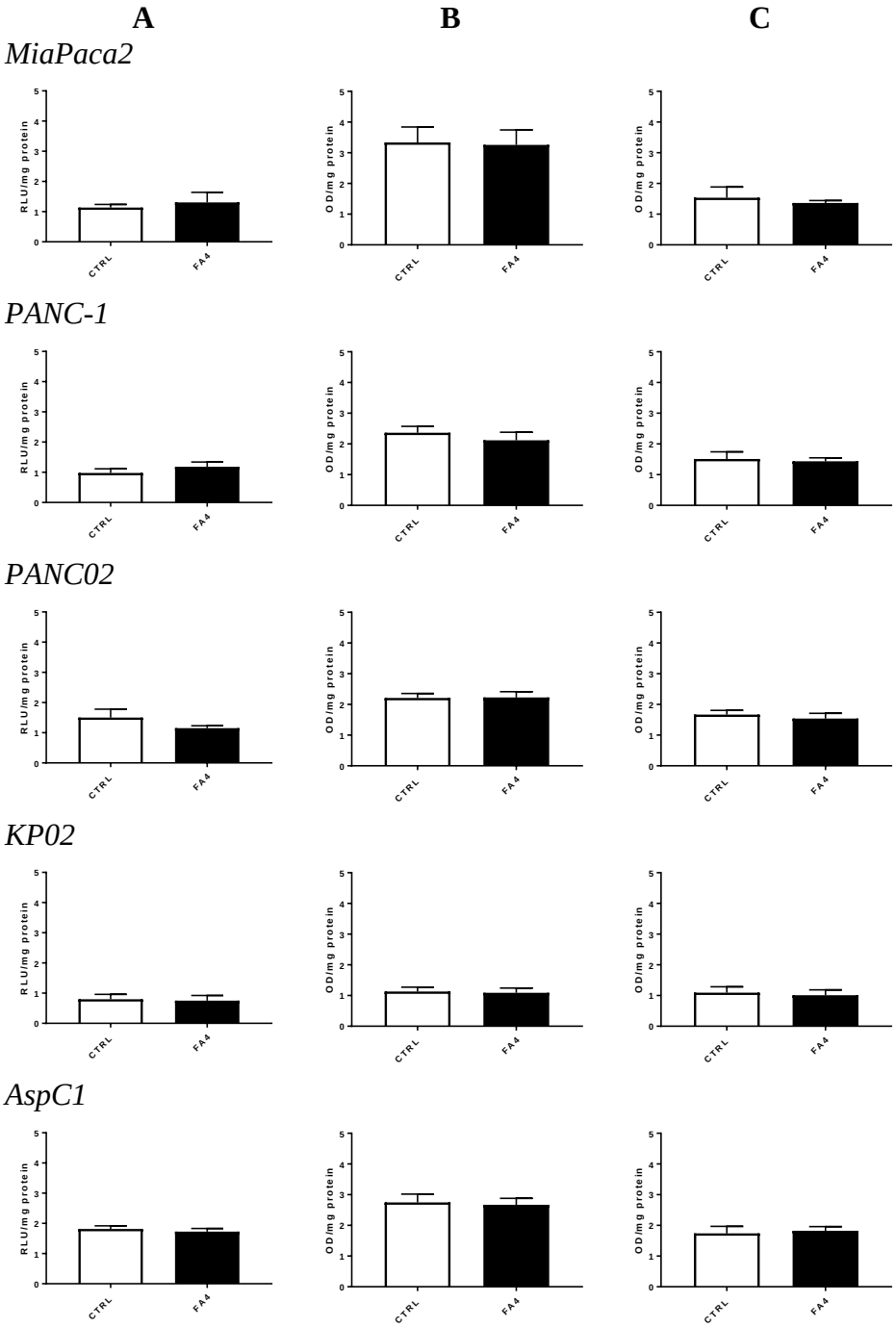

Figure S5. FA4 efficacy against PANC-1 and MiaPaCa2 xenografts. FA4 in C57BL/6 mice bearing PANC-1 (panel A) or MiaPaCa2 (panel B) tumors, treated for 15 days as follows: 1) Vehicle group (black line, 100 µL saline solution); 2) FA4^{low} group (red line, 750 nmoles FA4 in 100 µL saline solution); 3) FA4^{high} group (yellow line, 1500 nmoles FA4 in 100 µL saline solution); 4) Gemcitabine group (green line, 20 mg/kg gemcitabine, twice a week). Animals were euthanized at day 18. Results are means ± SEM (n = 8). ***P<0.001: FA4-groups *vs* vehicle (day 18); $^{\#}$P<0.05, $^{\#\#}$P<0.001; FA4-groups *vs* gemcitabine (day 18).